Theses and Dissertations | 1. Thesis and Dissertation Collection, all items

1991-06

Ambient sound in the ocean induced by heavy precipitation and the subsequent predictability of rainfall rate

McGlothin, Charles C. Jr.

Monterey, California. Naval Postgraduate School

http://hdl.handle.net/10945/26348

NAVAL POSTGRADUATE SCHOOL
Monterey, California

THESIS

AMBIENT SOUND IN THE OCEAN INDUCED BY
HEAVY PRECIPITATION AND THE SUBSEQUENT
PREDICTABILITY OF RAINFALL RATE

by

Charles C. McGlothin, Jr.

June, 1991

Thesis Advisor: Jeffrey A. Nystuen

Approved for public release; distribution is unlimited

REPORT DOCUMENTATION PAGE

1a. REPORT SECURITY CLASSIFICATION UNCLASSIFIED	1b. RESTRICTIVE MARKINGS
2a. SECURITY CLASSIFICATION AUTHORITY	3. DISTRIBUTION/AVAILABILITY OF REPORT
2b. DECLASSIFICATION/DOWNGRADING SCHEDULE	Approved for public release; distribution is unlimited.

4. PERFORMING ORGANIZATION REPORT NUMBER(S)	5. MONITORING ORGANIZATION REPORT NUMBER(S)

6a. NAME OF PERFORMING ORGANIZATION Naval Postgraduate School	6b. OFFICE SYMBOL (If applicable) 55	7a. NAME OF MONITORING ORGANIZATION Naval Postgraduate School
6c. ADDRESS (City, State, and ZIP Code) Monterey, CA 93943-5000		7b. ADDRESS (City, State, and ZIP Code) Monterey, CA 93943-5000

8a. NAME OF FUNDING/SPONSORING ORGANIZATION	8b. OFFICE SYMBOL (If applicable)	9. PROCUREMENT INSTRUMENT IDENTIFICATION NUMBER

8c. ADDRESS (City, State, and ZIP Code)	10. SOURCE OF FUNDING NUMBERS			
	Program Element No	Project No.	Task No	Work Unit Accession Number

11. TITLE (Include Security Classification)
Ambient Sound in the Ocean Induced by Heavy Precipitation and the Subsequent Predictability of Rainfall Rate

12. PERSONAL AUTHOR(S) McGlothin, Charles C., Jr.

13a. TYPE OF REPORT Master's Thesis	13b. TIME COVERED From To	14. DATE OF REPORT (year, month, day) June 1991	15 PAGE COUNT 78

16. SUPPLEMENTARY NOTATION
The views expressed in this thesis are those of the author and do not reflect the official policy or position of the Department of Defense or the U.S. Government.

17. COSATI CODES			18. SUBJECT TERMS (continue on reverse if necessary and identify by block number)
FIELD	GROUP	SUBGROUP	Rainfall Rate, Underwater Sound Spectrum, Algorithm, Ambient Sound, Heavy Precipitation

19. ABSTRACT (continue on reverse if necessary and identify by block number)

An experiment by the Naval Postgraduate School and the National Data Buoy Center was preformed in the Gulf of Mexico to characterize the underwater sound generated by heavy precipitation and to determine if rainfall rate can be measured using underwater sound. During this stage of the esperiment, twenty-two data sets were recorded with rainfall rates up to 340 mm/hr. For a given rainfall rate, it is found that sound levels from heavy convective precipitation are higher at the beginning of the storm and when rainfall rate is increasing than at the end of the storm event or when rainfall rates are decreasing. This may be due to changes in the drop size distribution during the life cycle of the storm or to variations in the temperature difference between the raindrop and the ocean surface. Very heavy rainfall (> 150 mm/hr) generates near surface bubble layers or bubble clouds which attenuate sound energy at higher frequencies (> 15 kHz). The distinctive 15 kHz peak in the sound spectrum for light rain is absent during heavy rain suggesting that the sound production mechanism previously identified for small drops (0.8 - 1.1 mm in diameter) is suppressed by heavy rain even though those small drops are undoubtedly present during heavy rainfall rates. These data show a very high correlation between underwater sound level and the logarithm of the rainfall rate except when high wind speeds (> 10 m/s) and high rainfall rates (> 150 mm/hr) are present. An empirical rainfall rate algorithm for convective precipitation is proposed suggesting that sound energy is directly proportional to rainfall rate, however any empirical algorithm which does not adjust for changing storm characteristics should be used with caution.

20. DISTRIBUTION/AVAILABILITY OF ABSTRACT			21. ABSTRACT SECURITY CLASSIFICATION
☒ UNCLASSIFIED/UNLIMITED	☐ SAME AS REPORT	☐ DTIC USERS	Unclassified
22a. NAME OF RESPONSIBLE INDIVIDUAL Jeffrey A. Nystuen		22b. TELEPHONE (Include Area code) (408) 646-2917	22c OFFICE SYMBOL OC/Ny

DD FORM 1473, 84 MAR   83 APR edition may be used until exhausted   SECURITY CLASSIFICATION OF THIS PAGE
All other editions are obsolete   Unclassified

Ambient Sound in the Ocean Induced by
Heavy Precipitation and the Subsequent
Predictability of Rainfall Rate

by

Charles C. McGlothin, Jr.
Lieutenant, United States Navy
B.S., Mississippi State University, 1982

Submitted in partial fulfillment
of the requirements for the degree of

MASTER OF SCIENCE IN PHYSICAL OCEANOGRAPHY
AND METEOROLOGY
from the

NAVAL POSTGRADUATE SCHOOL
June 1991

ABSTRACT

An experiment by the Naval Postgraduate School and the National Data Buoy Center was performed in the Gulf of Mexico to characterize the underwater sound generated by heavy precipitation and to determine if rainfall rates of heavy precipitation can be measured using underwater sound. During this stage of the experiment, twenty-two data sets were recorded with rainfall rates up to 340 mm/hr. For a given rainfall rate, it is found that sound levels from heavy convective precipitation are higher at the beginning of the storm and when the rainfall rate is increasing than at the end of the storm event or when rainfall rates are decreasing. This may be due to changes in the drop size distribution during the life cycle of the storm or to variations in the temperature difference between the raindrop and the ocean surface. Very heavy rainfall (rate > 150 mm/hr) generates near surface bubble layers or bubble clouds which attenuate sound energy at higher frequencies (>15 kHz). The distinctive 15 kHz peak in the sound spectrum for light rain is absent during heavy rain suggesting that the sound production mechanism previously identified for small drops (0.8 - 1.1 mm in diameter) is suppressed by heavy rain even though those small drops are undoubtedly present during heavy rainfall rates. These data show a very high correlation between underwater sound level and the logarithm of the rainfall rate except when high wind speeds (> 10 m/s) and high rainfall rates (> 150 mm/hr) are present. An empirical rainfall rate algorithm for convective precipitation is proposed suggesting that sound energy is directly proportional

to rainfall rate, however any empirical algorithm which does not adjust for changing

storm characteristics should be used with caution.

TABLE OF CONTENTS

vi

LIST OF TABLES

LIST OF FIGURES

ACKNOWLEDGEMENT

I. INTRODUCTION

The measurement of precipitation is an important parameter in the climatological system and is critical for forecasting accurate weather. It is, however, a very difficult measurement to make. Rain gauges, though limited in value because of sampling difficulties, do provide a measurement of precipitation over land. Over the ocean (71% of the earth's surface), precipitation measurements are only known at locations (ships, buoys, oil platforms) where some type of rain gauge has been installed. These precipitation measurements are qualitatively useful, but rain gauge inaccuracies affected by disturbances of air flow over the platform seriously affect the quality of the observations. Platforms that are not "stable" (solidly mounted to the ocean's floor) are also subjected to additional uncertainties caused by the platform's motion. Satellite techniques have been proposed to measure precipitation over the ocean, but the methods lack surface verification at present. Eventually, they are likely to play an important role.

An excellent candidate for a method of measuring rainfall in oceanic regions is to monitor the underwater sound produced by precipitation. The detection and measurement of precipitation over the ocean could be accomplished by remote sensors (bottom mounted or free drifting) which are not affected by, and do not interfere with, the surface processes being measured. Recently an algorithm for the measurement of wind (another known source of ocean ambient noise) using ambient noise has been proposed (Vagle *et al.*, 1990). Much less is known about ambient noise generated by precipitation, however

1

work continues exploring the viability of making precipitation measurements using the acoustic signature of the ambient noise in the ocean. An algorithm to predict rainfall rate has not yet been developed because of influences of air/sea conditions on the rain generated sound spectrum are not fully understood.

Figure 1 shows a representative spectrum for a variety of ambient noise sources in
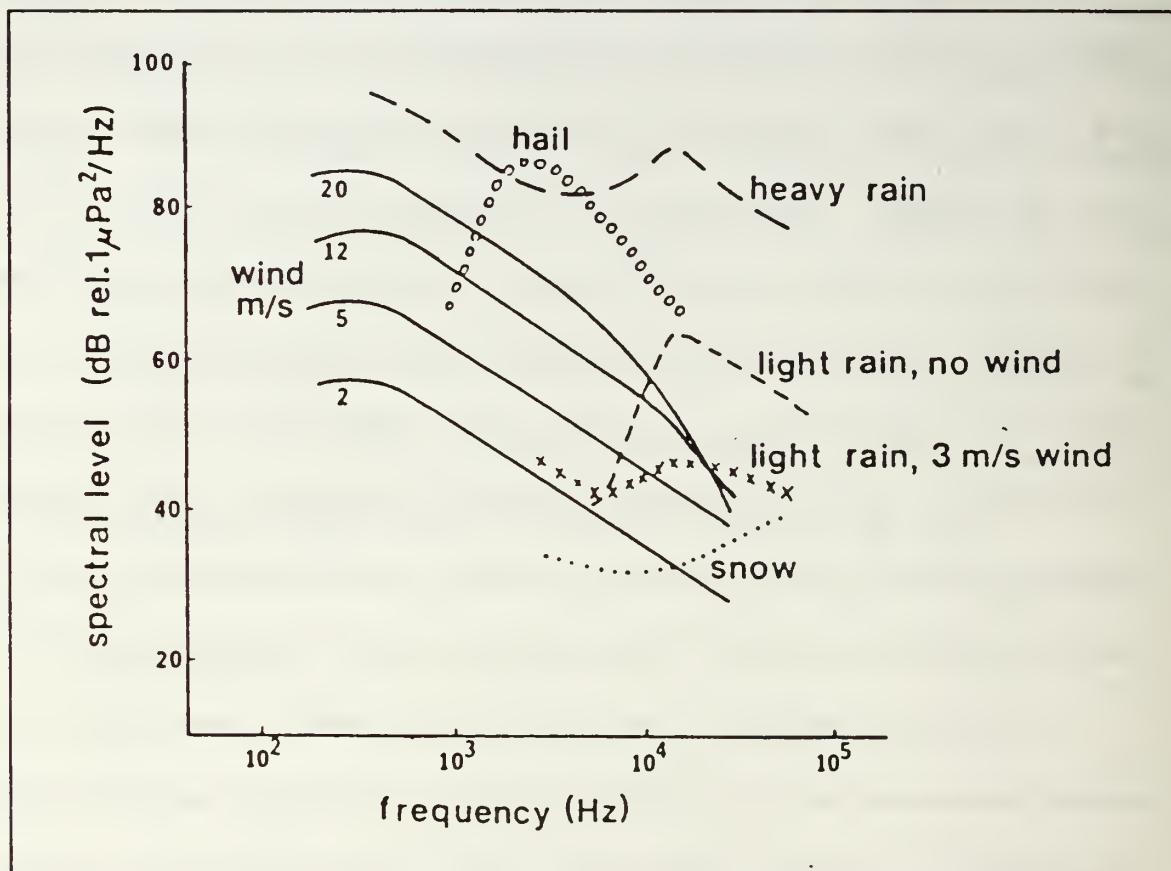
Figure 1. Spectral characteristics of ocean noise (Nystuen and Farmer, 1989).

the ocean. Precipitation, particularly rain, is shown over a frequency range of 1 to 30 kHz. Its shape is distinctively different from that of the wind, which allows the separation of the two sources. Noise generated by wind is though to be a product of bubbles generated by breaking waves (Knudsen *et al.*, 1948; Farmer and Vagle, 1988;

2

Medwin and Beaky, 1989). Ambient noise and wind speed has been shown to be highly correlated at 4.3, 8 and 14.5 kHz (Farmer and Lemon, 1984; Evans *et al.*, 1984; Vagle *et al.*, 1990) and yields a logarithmic relationship when wind speed is between 0 and 12 m/s. At wind speeds greater than 10 m/s, a subsurface bubble layer forms and attenuates surface generated noise at higher frequencies (greater than 10 kHz) (Farmer and Lemon, 1984; Farmer and Vagle, 1988).

Ambient noise produced by precipitation has received much attention recently (Nystuen and Farmer, 1987, 1989; Scrimger *et al.*, 1989), especially ambient noise produced in light wind and light precipitation conditions (Nystuen, 1991). Identification of the source mechanisms during these events have been extensively studied (Pumphrey *et al.*, 1989), but have been limited to small raindrop sizes at near normal angles of impact, i.e., light wind conditions. In turn, these studies provide insight into precipitation sound generated by natural rainfall, but attempts at prediction of precipitation would be constrained to light wind/light rain conditions. Precipitation, in general, does not have a constant, small drop size nor does the wind conditions remain light, especially in convective precipitation.

A rain drop produces underwater sound from the initial impact and a subsequent bubble. If the bubble is created, it dominates the sound field. Figure 2 (Kurgan 1989) (or Medwin *et al.*, 1990) shows the sound pressure produced by the initial impact and the bubble for a 0.83 mm diameter drop. The energy produced by the bubble is approximately 200 times that produced by the impact. The probability of creation of a subsequent bubble depends on drop size and impact geometry (Medwin *et al.*, 1990). For
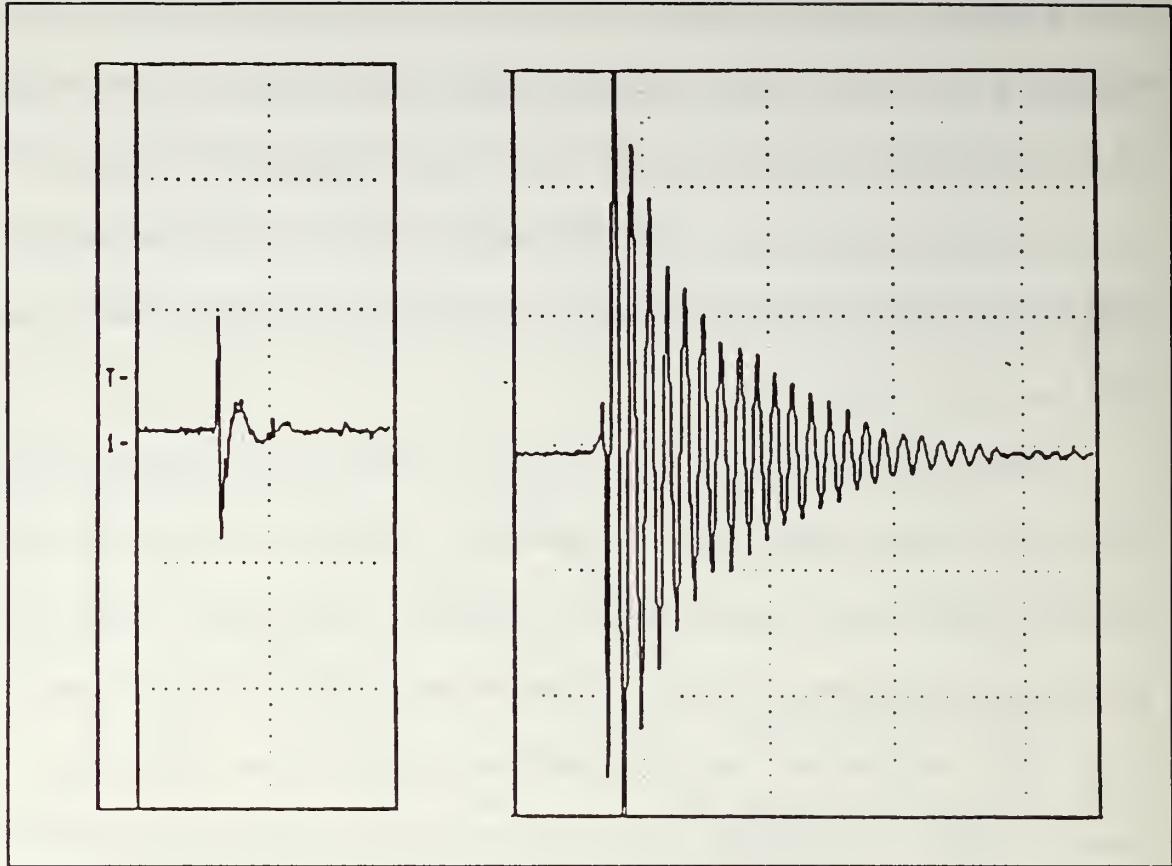
Figure 2. Pressure signal from the impact sound (left) and the bubble sound (right) produced by a 0.83 mm diameter drop at normal incidence and terminal velocity. The time scale is 400 μs per division (Kurgan, 1989).

natural raindrops sizes falling at terminal velocities, two size ranges with two distinctive bubble creation mechanisms have been identified (Figure 3). Type I bubbles are generated at the apex of the conical splash crater (Pumphrey, 1990) and Type II bubbles are generated as a turbulent jet, created during the splashes, plunges through the bottom of the hemispherical splash crater (Snyder, 1990).

The sound generated by Type I drops (drop sizes: 0.8 - 1.1 mm in diameter) has been extensively studied. These drop sizes are almost always present in nature rain and would be expected to entrain bubbles. The size of the entrained bubbles causes them to

4
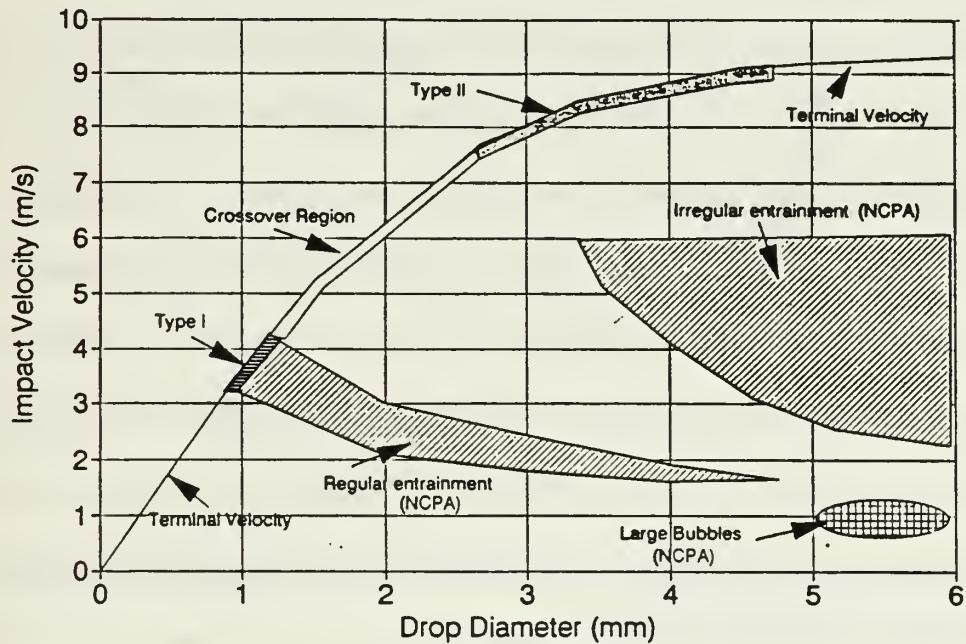
Figure 3. The shaded region (regular entrainment) shows the parameters (drop size and impact velocity) necessary for entrainment to occur. The curve on the left shows the terminal velocity for falling drops in still air (Courtesy of P. W. Jacobus).

be resonant at 14 kHz. This explains why the 14 kHz peak is present for precipitation containing these drop sizes (Figure 4). In fact, under light and no wind conditions with rainfall containing only small drops (drop sizes < 1.5 mm diameter) a well defined peak is observed at approximately 14 kHz. However the conditions required to create a bubble are very specific: flat surface and normal incidence. The bubble entrainment mechanism is sensitive to the incident angle of the rain drop impact (Medwin *et al.*, 1990) so that little increases in wind speed (1 - 3 m/s) and/or roughing of the sea surface drastically reduces the probability of entrainment. This fact is used to explain the suppression

5
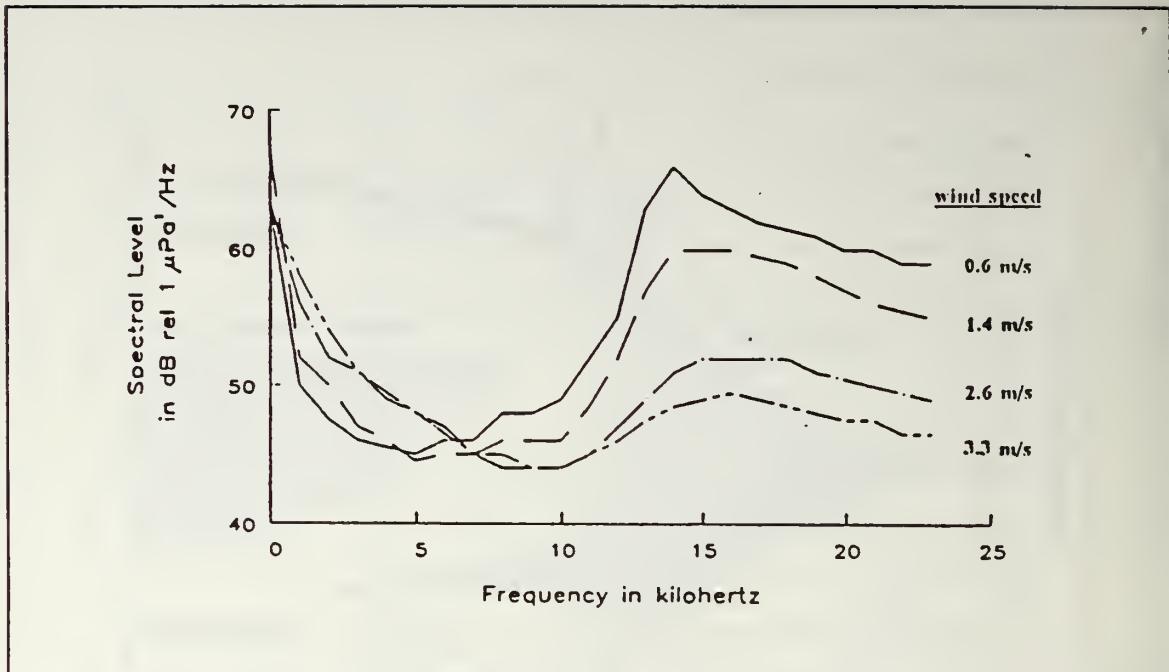
Figure 4. Sound spectra generated under low rainfall rate (0.6 mm/hr) and different wind speeds (Nystuen and Farmer, 1987).

observed of the spectral of peak as the wind increases (Figure 4) (Nystuen, 1990).

Although small raindrops are an important source of sound under very specific conditions, they generally do not contribute much volume to the total rainfall rate. Rainfall rate is the volume of rain water falling per unit time per unit area and is defined as:

$$RR = C \int_{d=200\mu m}^{d=5mm} DSD * V_t * (\frac{\pi * d^3}{6}) \, dd \qquad (1)$$

where RR is rainfall rate (mm/hr), C is unit conversion constant (m^2/mm^2), DSD is drop size distribution (#/m^3 mm), V_t is terminal velocity (m/s) and d is drop diameter (mm). The terminal velocity is approximately proportional to $d^{1/2}$, therefore RR is the $d^{7/2}$ th moment of the DSD. This means large drops usually contain most of the water volume

6

in rain and so identifying their role in underwater sound production is critical to a relationship between rainfall rate and sound levels. As rainfall rate increases, the number of all drop sizes increases, but proportionally the number of large drops increases faster than the number of smaller drops (Pruppacher and Klett, 1978).

This paper will describe the characteristics of ambient sound generated by heavy precipitation (presumably containing large drops) and describe the correlation between rainfall rate and ambient sound. Time evolution of the sound generated by convective precipitation is characterized in an effort to yield insight into the prediction of rainfall rate based on acoustical measurements. The data used is from an ongoing experiment at the Ocean Test Platform (OTP) in the Gulf of Mexico. This experiment records acoustic data along with associated environmental conditions when the rainfall rate exceeds 10 mm/hr. This rainfall rate is enough to ensure the presence of large drop sizes (Rogers and Yau, 1976).

II. DATA ACQUISITION AND PROCESSING

A. EXPERIMENT LOCATION AND EQUIPMENT ARRANGEMENT

This study is part of the Ambient Noise Drifting Buoy Program being conducted by the National Data Buoy Center (NDBC) and the Naval Postgraduate School (NPS) to understand the sound generated by heavy precipitation under varying meteorological and oceanic conditions. The experiment was conducted at NDBC's Ocean Test Platform (OTP) in the Gulf of Mexico about 40 kilometers off the coast of Mississippi (Figure 5).
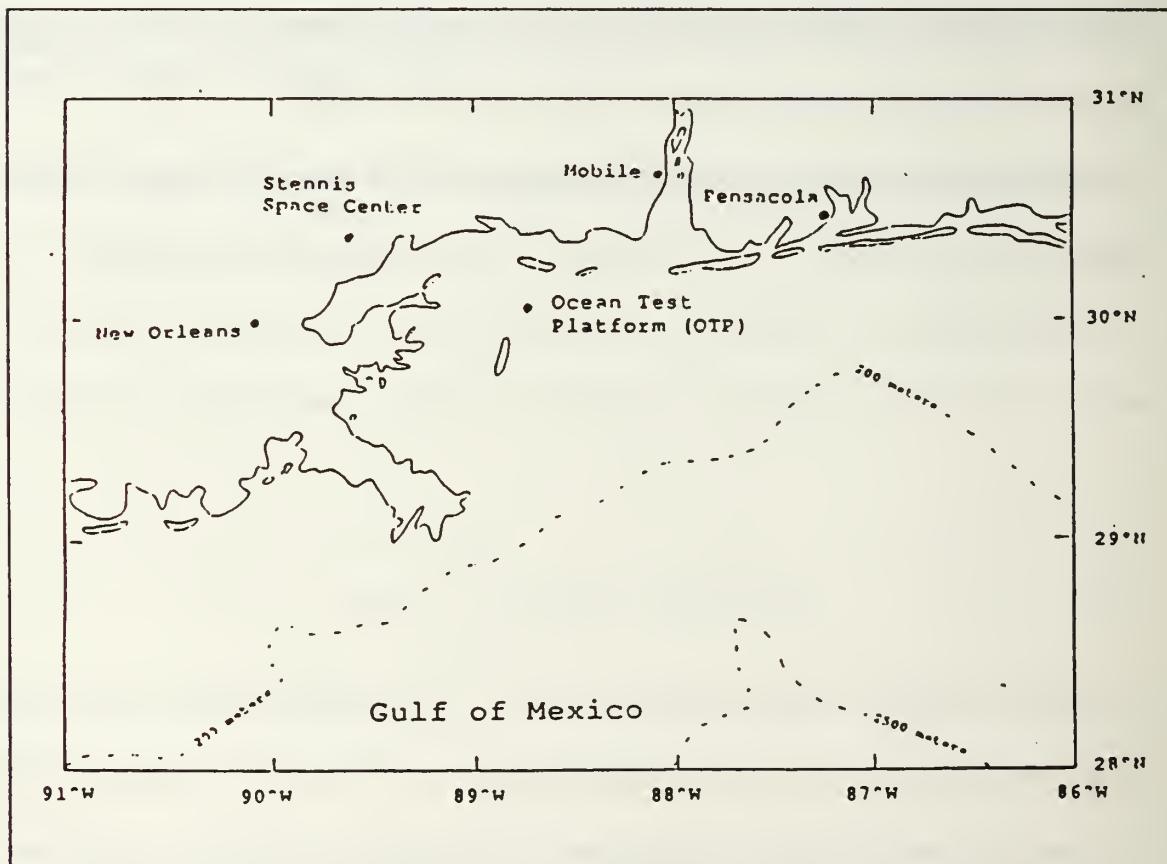
Figure 5. Location of Ocean Test Platform (OTP) (Tan, 1990).

8

The OTP is a permanently moored buoy (10 meters in diameter) in 15 meters of water (Figure 6). The data acquisition system consists of a hydrophone, recorder, optical

1. OPTICAL RAIN GAUGE
2. WIND SPEED SENSOR
3. RAIN ACCUMULATION SENSOR
4. DIRECTIONAL WAVE MEASURING SYSTEM
5. DAT RECORDER, MODEL 6 DATA LOGGER
6. HYDROPHONE CABLE
7. HYDROPHONE
8. HYDROPHONE SUPPORT FIXTURE
9. ANCHOR CHAIN (3-POINT MOOR)
10. 6000 LBS ANCHOR
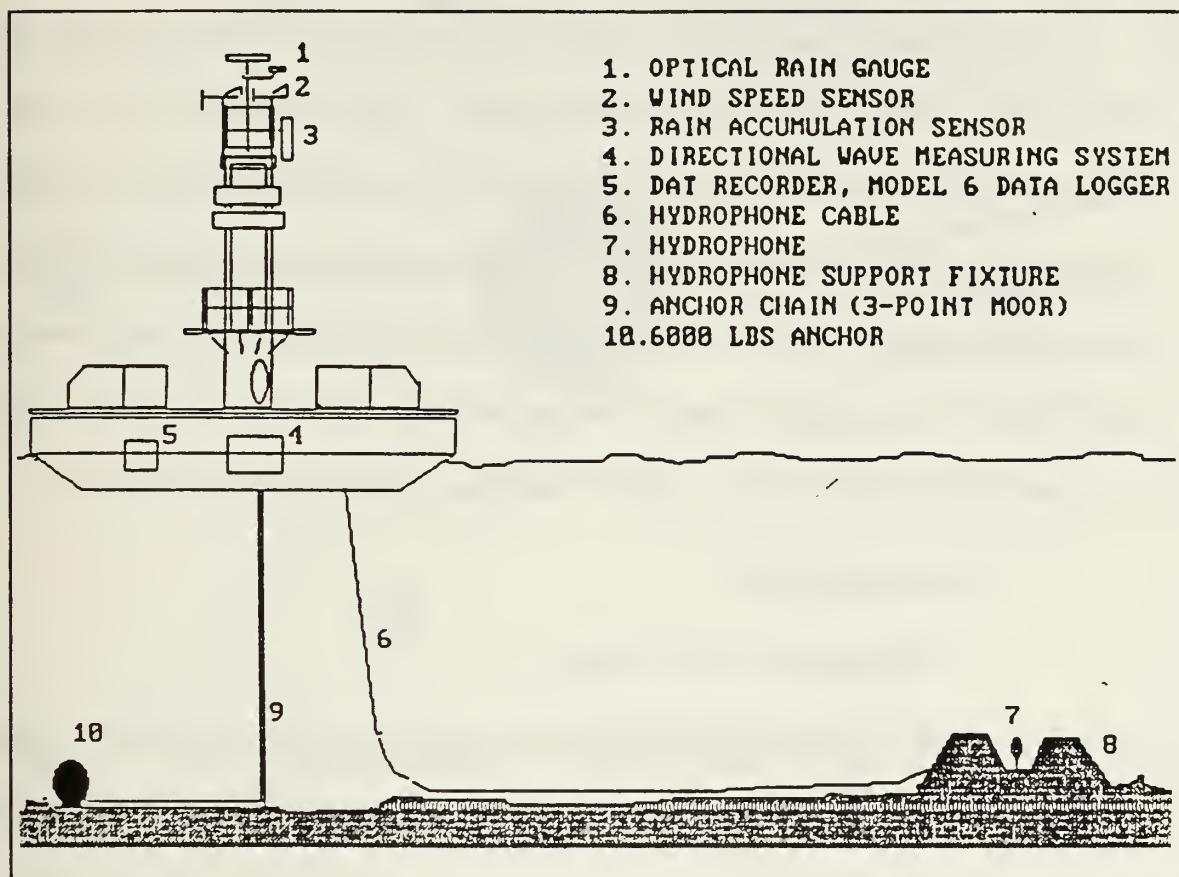
Figure 6. Ocean Test Platform (OTP) equipment arrangement (Tan, 1990).

and accumulation rain gauges and anemometer. Measurements of ocean surface conditions including wind speed and direction, wave height and direction, air and sea temperatures and precipitation are automatically recorded and reported via the GOES satellite communication link to NDBC. Weather radar coverage is provided by the National Weather Service by the radar site located at Slidell, LA.

9

B. EQUIPMENT

1. Acoustic Data

A ITC Model 3001 hydrophone modified to incorporate a 23 dB preamplifier was used to collect digital recordings of ambient sound. The hydrophone was set into a cement block on the ocean bottom (water depth of 13 meters) approximately 70 meters from the OTP. The hydrophone has a narrow upward looking beam pattern (30°). This beam pattern together with the distance from the OTP expected to reduce noise from the buoy (Figure 7). The acoustic data was transmitted to the OTP via cable and recorded on a Model TCD-D10 PRO Sony Digital Audio Tape recorder (DAT) at 44,100 Hz.

2. Environmental Data

a. *Precipitation Measurements*

A RM Young Model 50202 rain accumulator sensor (siphon rain gauge) was used to measure the total accumulated rainfall. A Scientific Technology, Inc optical rain gauge Model ORG-705C was used to measure the rainfall rate. The optical rain gauge and the rain accumulator sensor has a 0 - 5 VDC analog output which was fed directly to the data logger. The optical rain gauge has 1% accuracy over the range of 10 to 100 mm/hr, a 4% accuracy over the range of 1 to 500 mm/hr and a 10% accuracy over the range of 0.5 to 1000 mm/hr. The optical rain gauge has an internal 10 second exponential average. The siphon rain gauge is an experimental design which has an accuracy of ± 2 mm over threshold of 1 mm with a smoothing filter of 10 seconds. The measuring range for the siphon rain gauge is 0 - 50 mm where 0 - 5 VDC represents 0 -
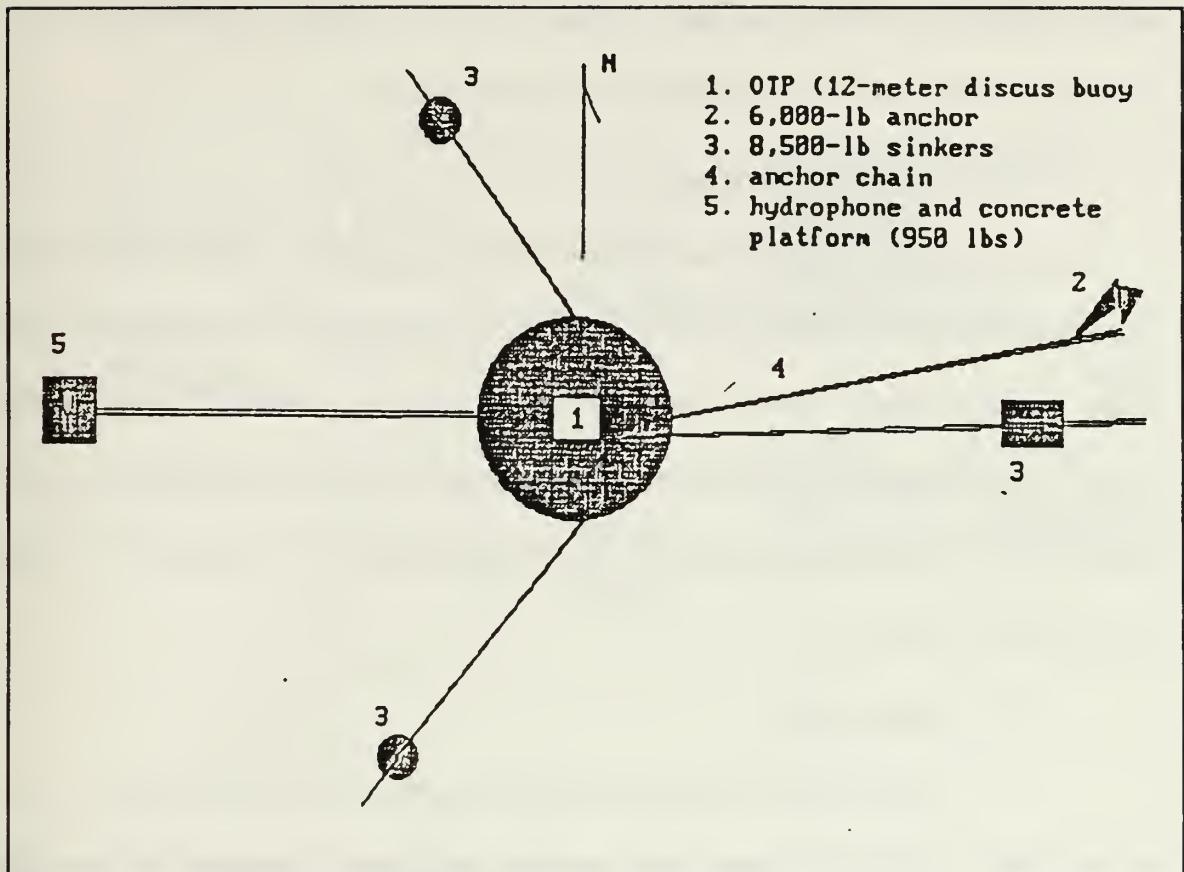
Figure 7. OTP mooring arrangement. The hydrophone (5) lies 270° T from the OTP buoy (1) (Tan, 1990).

50 mm. Both gauges were installed at the 10 meter level on the buoy and monitor precipitation continuously. The acoustic recording system was preset to activate when the optical rain gauge indicated that the rainfall rate was greater than or equal to 10 mm/hr.

b. *Wind Measurements*

A RM Young Model 05203 - 1R wind monitor with tachometer generator was used to record the wind speed and direction when the acoustic data was being recorded. The instrument was installed at the 10 meter level and produce a 0 - 14 VDC

output which was buffered through a voltage divider (to limit the output to 5 volts maximum for the data logger) and fed into the data logger.

c.   *Wave Measurements*

The OTP buoy has two wave measuring systems which report hourly wave data through the GOES satellite network. Wave spectral data, significant wave height and wave period data are available and are archived at the NDBC Computer Center. The time series wave data (i.e., corresponding with the environmental time series data) was not used since the buoy had a 3 point mooring which invalidated previously wave sensor calibrations.

d.   *Radar Data*

Meteorological radar data was provided by the National Weather Service for the OTP. Local weather plots were provided at 15 minute intervals when available and when the acoustic recording system was activated. These NOWRAD images printed by "WX - VIEW" from Robertson software provided 1 - 6 levels of echo intensities. These plots provide a reference for comparison with in-situ rainfall rate measurements and show storm type and coverage.

e.   *Data Logger*

The Model 6 A/D data logger is from a 12 bit A/D converter with a 5 volt reference and a 200 megabyte data storage capability where a 0 - 5 VDC input signal was represented by 0 - 4095 counts. Figure 8 shows the control diagram for environmental and acoustic data acquisition.
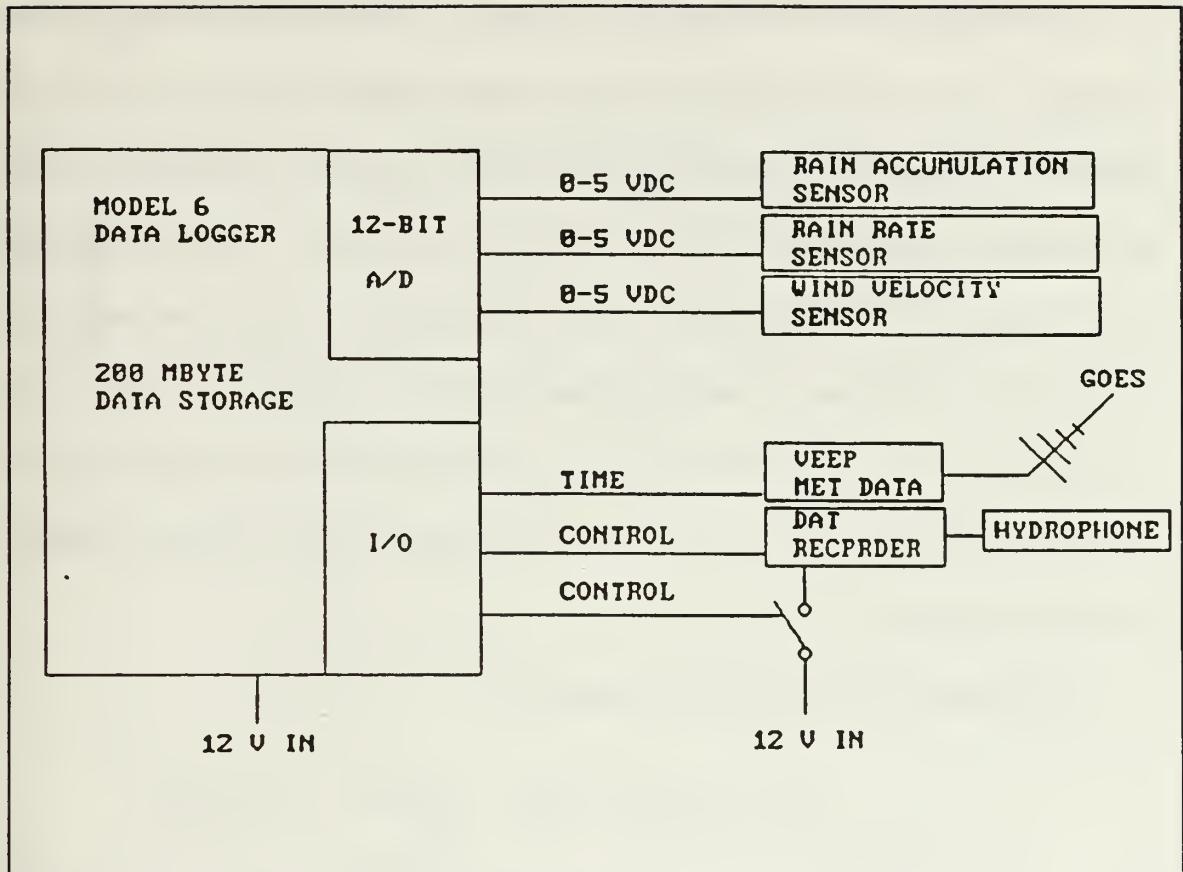
Figure 8. Control diagram of the experiment equipment (Tan, 1990).

C. DATA PROCESSING

The processing of the digitally recorded acoustic data was accomplished at NPS by converting the digital signal to a sound spectrum. By using a Sony Digital Pulse Code Modulator (PCM), the raw acoustic signal on the DAT tape was transferred to a HP computer using a program containing a Fast Fourier Transform (FFT) algorithm which completed the conversion to a sound spectrum. Further processing occurred after transferring these data to an IBM PC.

13

The program used contained several checks to ensure the signal was processed accurately. The variance of the acoustic energy output from the PCM was calculated and compared to the energy spectrum output from the FFT. The PCM used was designed for audio signals and contained a filter which shifted the amplitude of the signal depending on the frequency. To correct for this amplitude change along with any variations in the DAT recorder and/or tape, an amplitude filter function was designed using white noise. Test tones were recorded on each data tape at 5, 10, 15 and 20 kHz. These 3 milliVolt test tones were used to verify signal output of the system along with initially adjusting the filter coefficient.

The equation for the conversion process is:

$$SL = 10 * Log_{10} \left[\frac{Cf\left(\frac{Volts^2}{Counts^2}\right) * Sp\left(\frac{Counts^2}{\Delta f}\right) * Ch\left(\frac{\mu Pa^2}{Volts^2}\right)}{Delf\left(\frac{Hz}{\Delta f}\right)} \right] \quad \textbf{(2)}$$

where SL is the sound spectral level in dB rel to 1 μPa^2/Hz, Cf is the processing equipment sensitivity correction factor (obtained from white noise voltage generator and test tones), Sp is the output of the FFT algorithm, Ch is the hydrophone sensitivity from the manufacturer and Delf is the bandwidth. The hydrophone sensitivity was reported from 5 to 20 kHz (Figure 9) from the manufacturer. The sensitivity curve was believed to be the source of some error (1 - 2 dB rel 1 μPa^2/Hz) in an earlier study and remains as such in this study. This is of special concern when determining absolute pressure levels, i.e., the fine details of the shape of the observed spectrum shown in Figure 10 is in doubt. These peaks, although varying in strength from case to case, were always
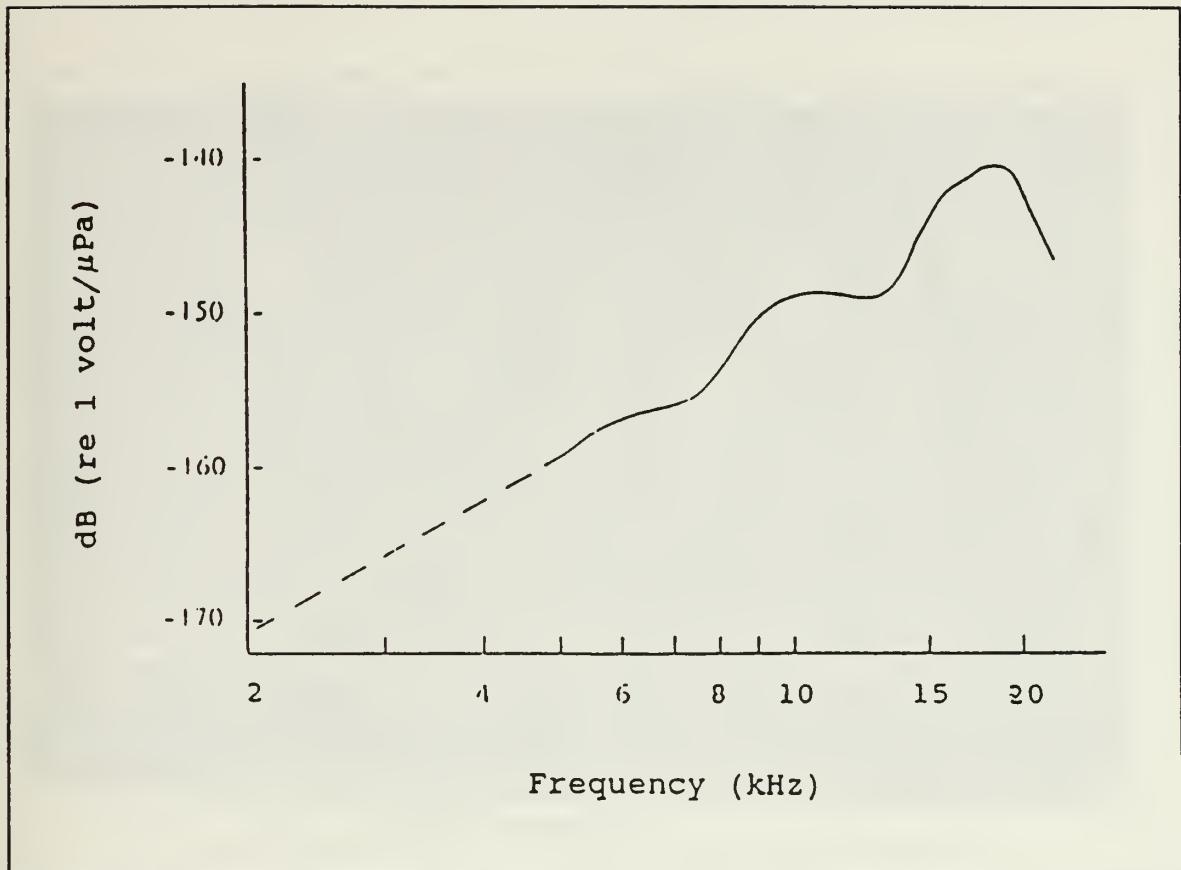
Figure 9. ITC Model 3001 hydrophone sensitivity curve.

present and could possibility be attributed to modified hydrophone sensitivity. Another

problems arose from extrapolation of the hydrophone sensitivity below 5 kHz. The

extrapolated sensitivity curve appears to produce sound levels higher than expected below

3 kHz. Consequently, all sound intensities below 3 kHz were considered suspect and are

not considered further. A calibration test is anticipated and should correct this situation

and will allow the use of these data at lower frequencies in future studies. This problem

does not affect the correlation between rainfall rate and sound level (i.e., it is a constant

offset in sound level).
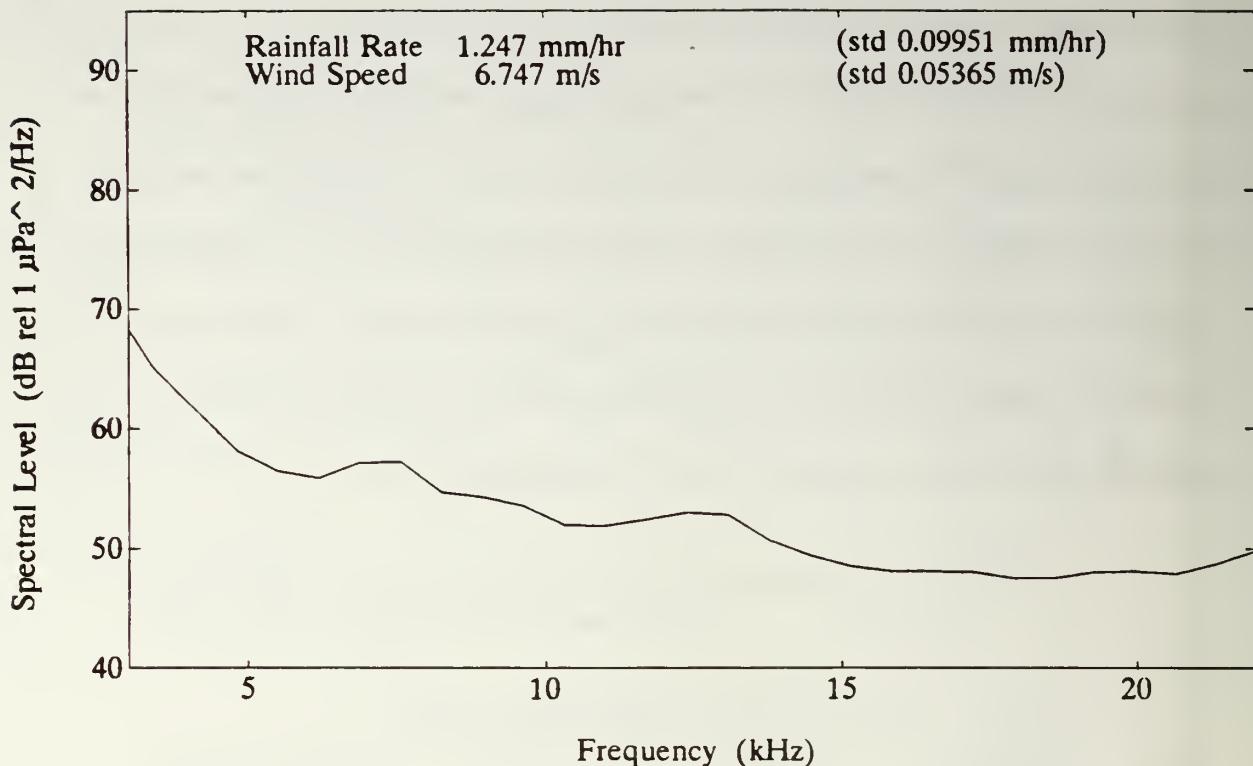
Figure 10. Example of sound level spectrum showing reoccurring structure approximately at 7 and 13 kHz which could possibility be attributed to the hydrophone sensitivity.

Two processing algorithms were designed to analyze the ambient sound data. One is an algorithm designed to analyze the ambient sound data using a 3-dimensional colored "waterfall" sonogram. In this display, the x-axis is the time series in seconds and the y-axis is frequency from 0 to 22.050 kHz with each color on the plot representing a different sound intensity level. This sonogram gives a visual representation of sound intensity and spectrum over a period of time which can be compared with the environmental data. An example is shown in Figure 11. The other algorithm was designed to process the raw digital acoustic signals to sound intensity levels as a function

16
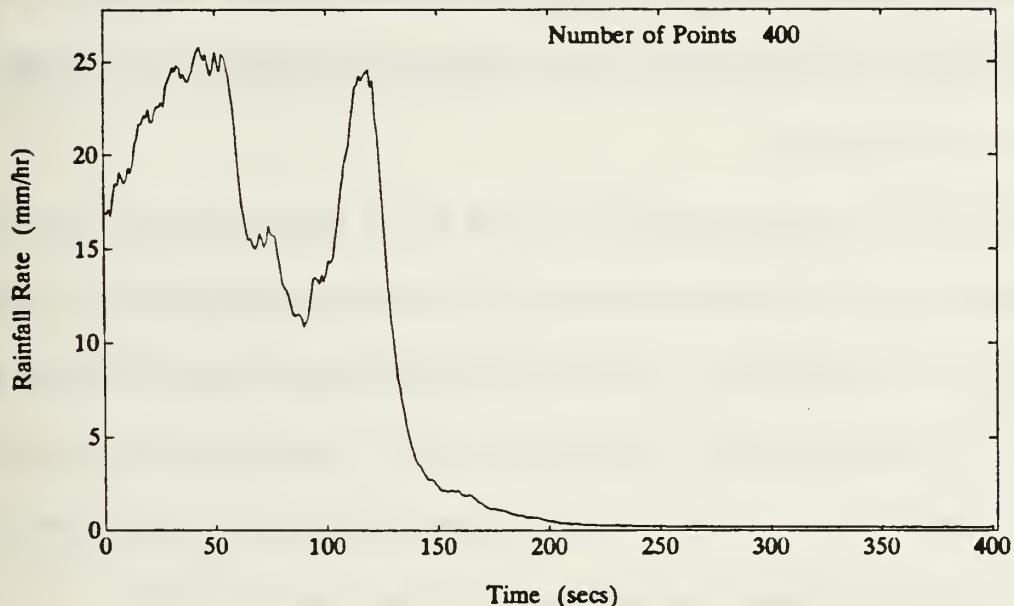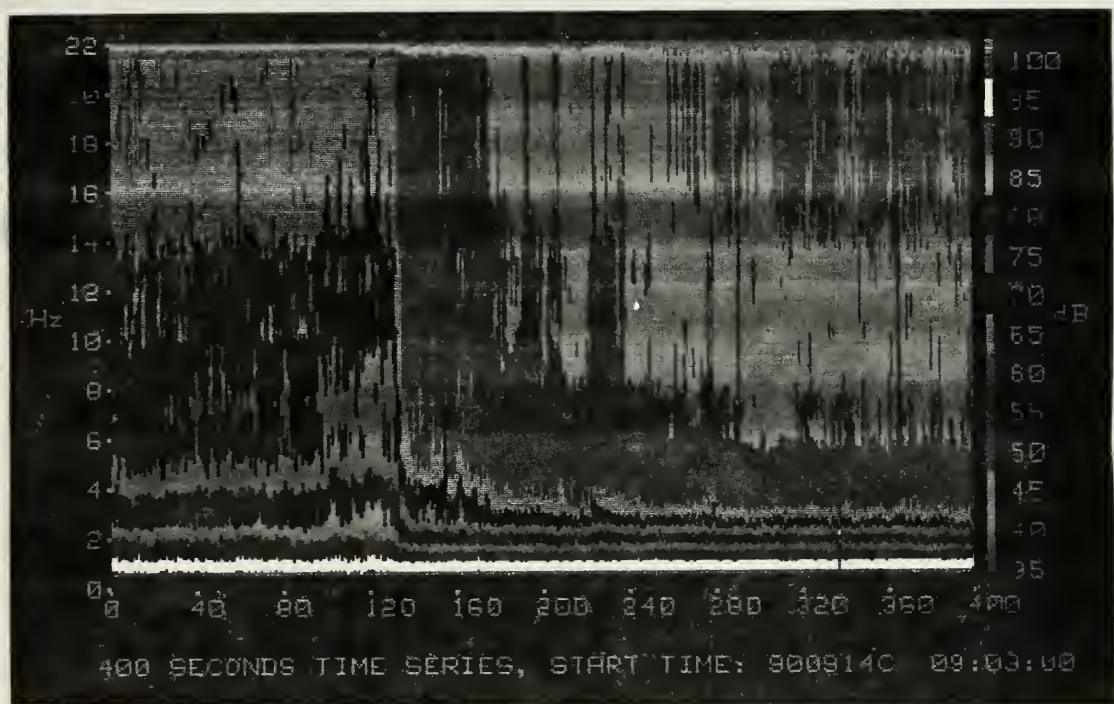
Figure 11. Sonogram (top) and rainfall rate time series (bottom) for event 900914C. Correlation coefficients were high (mean of 0.9852) for all frequencies between 3 and 22 kHz.

17

of frequency and time. These data were used to compute the correlations between intensity levels and versus environmental data (i.e., wind speed and direction, rainfall rate).

Several modes of either processing program could be used by changing the number of points in the FFT and/or the time step. A 64 point FFT was used to generate a time series with a time step of one second which could be directly compared to the environmental data. The tape recorder runs continuously while the computer alternates between reading and processing data during one second of real time. The higher the number of points in the FFT, the more time is required to read and process the data, thereby reducing the number of data iterations completed in one second (i.e., lower number of degrees of freedom). In the mode used, approximately 14 spectra are processed in one second of real data yielding 28 degrees of freedom. With the 64 point FFT, this program yielded spectra with 32 frequencies, each frequency having a bandwidth of 689.0625 Hz.

These data were then transferred to a IBM PC for further comparison with the environmental data. The optical rain gauge used a 10 second exponential filter to smooth the rainfall rate. Consequently, a 10 second exponential filter was used to smooth the wind speed and direction and the sound intensity levels. Figures 12 and 13 presents a example of the filtered wind speed and wind direction, respectively. Figure 14 shows a sound intensity time evolution in an unfiltered and filtered case at 5.51 kHz.
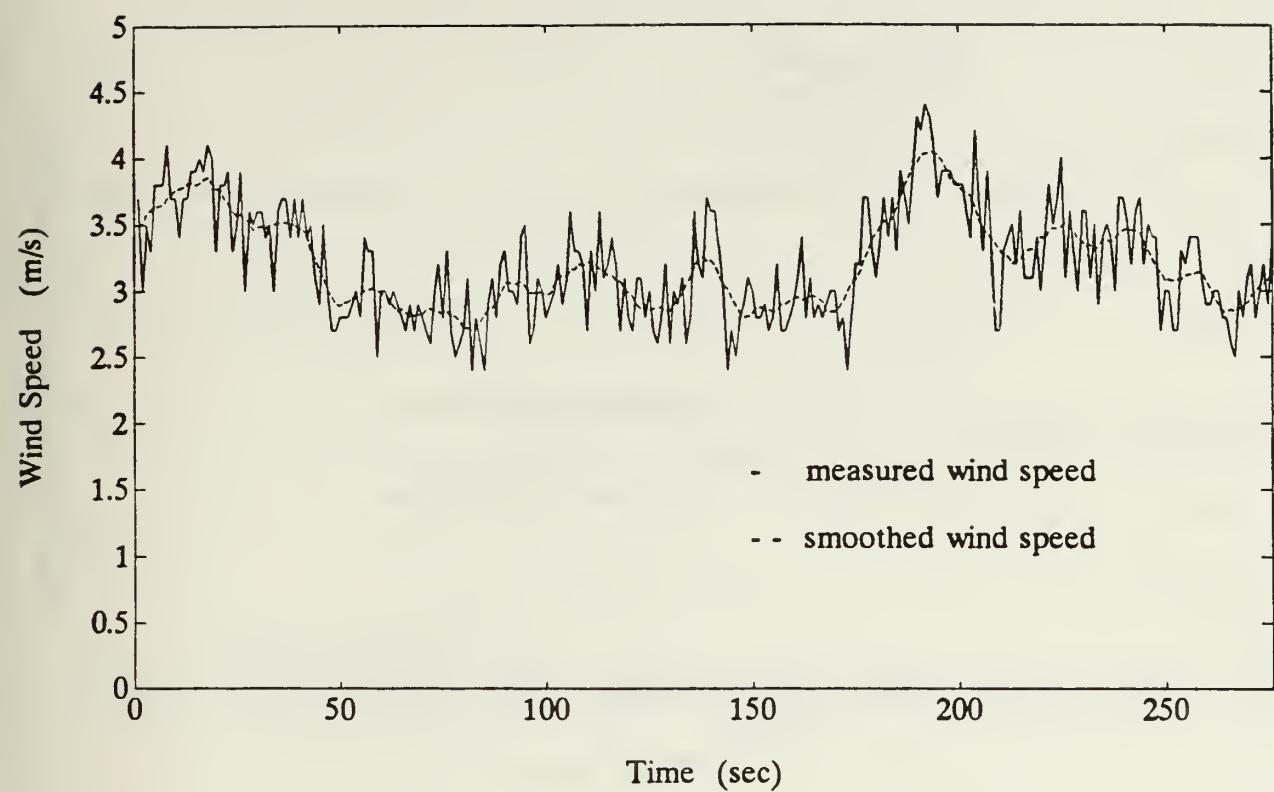
Figure 12. An example of wind speed in unfiltered and 10 second exponential filtered form.
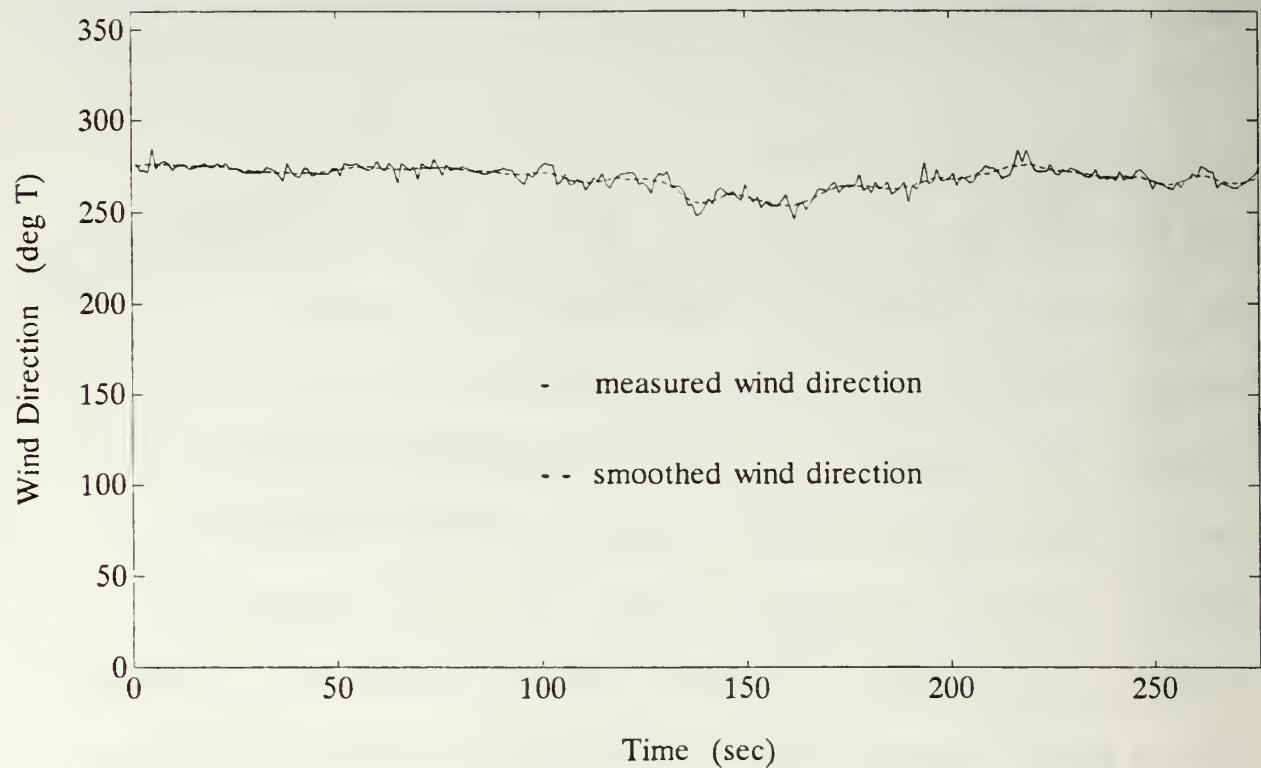
Figure 13. An example of wind direction in unfiltered and 10 second exponential filtered form.
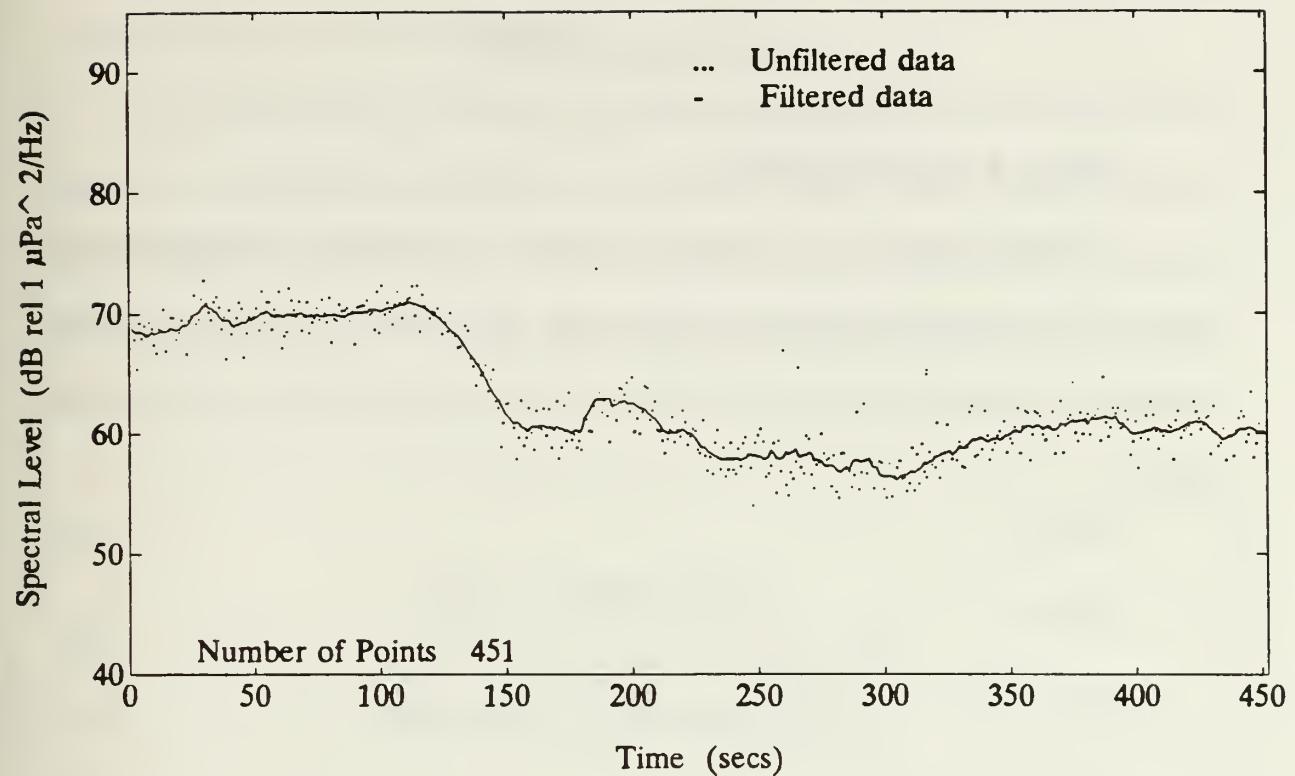
Figure 14. An example of time evolution of sound intensity at 5.5 kHz in an unfiltered and 10 second exponential filtered case.

21

III. DATA ANALYSIS

A. CORRELATION ANALYSIS

Correlation analysis is the attempt to measure the strength of the relationship between two variables by means of a single number. This number, the sample correlation coefficient, measures the linear association of one variable with the other. The equation used is:

$$r(i) = \frac{\sum_{t=1}^{n}(RR_t - \bar{RR})(SL(i)_t - \bar{SL}(i))}{\sqrt{\sum_{t=1}^{n}(RR_t - \bar{RR})^2 \sum_{t=1}^{n}(SL(i)_t - \bar{SL}(i))^2}} \tag{3}$$

where r is the sample correlation coefficient, i is frequency, n is the number of points in the time series, RR is the rainfall rate, SL is the sound spectral level and the bar over the variable indicates average value over the time period. Another form of the equation is:

$$r(i) = \frac{S_{RRSL_i}}{\sqrt{S_{RRRR}S_{SL_iSL_i}}} \tag{4}$$

where S is the covariance of the variable and all other variables being the same as in Equation (3). High values of correlation coefficients suggest probable predictability of rainfall rate from acoustic signals. Since the correlation coefficient is purely a measure

22

of their linear relationship, a correlation coefficient at or near zero simply implies a lack of linearity and not a lack of association.

Maximization of the correlation coefficients was achieved by calculating the cross-correlation coefficient at every point in time of the sound intensity with that to every point in time of the rainfall rate. This yielded a plot of correlation coefficients verses lag time (Figure 15). A positive lag means that the environmental data collection occurs after
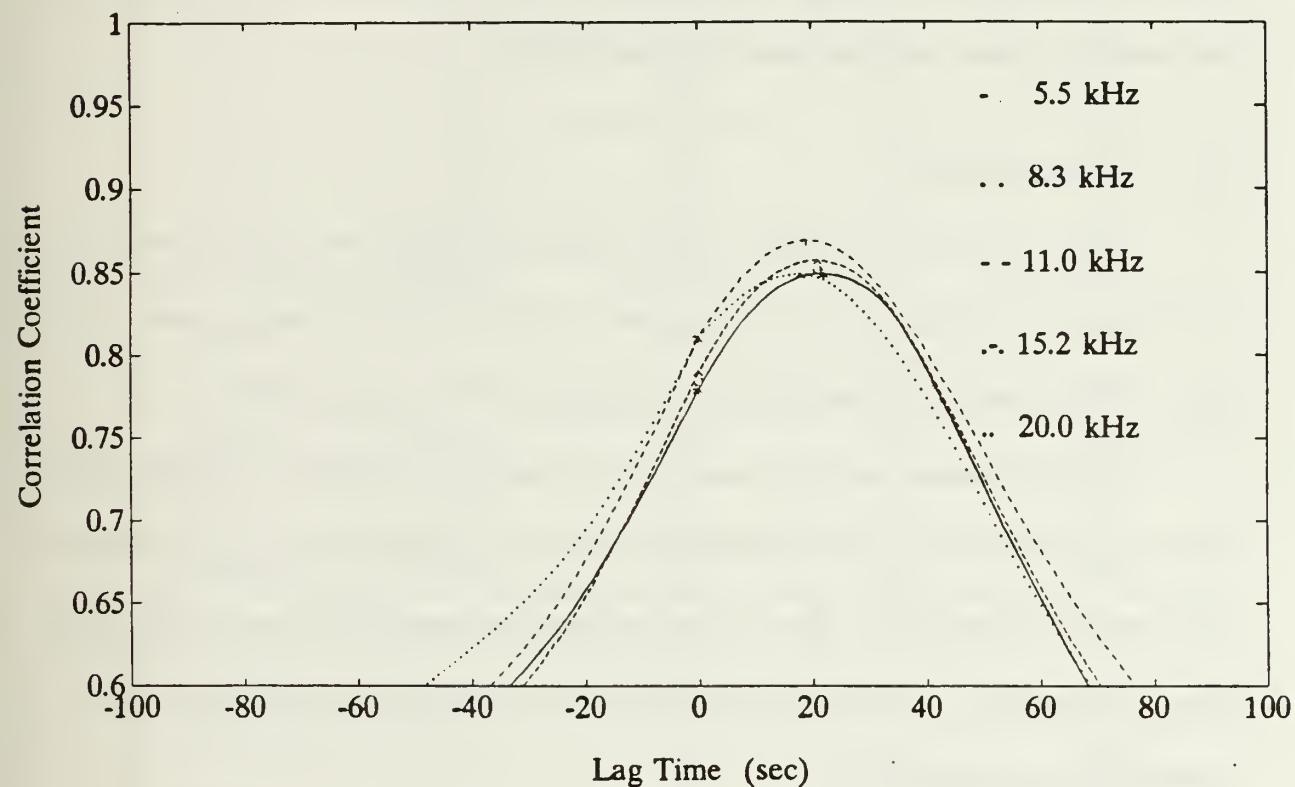
Figure 15. Cross-correlation between rainfall rate and sound intensity at 5 different frequencies for all times during the event.

the associated acoustic data collection. This lag is probably due to spatial or temporal variations in the storm events. All data sets were adjusted according to the calculated lag

times for maximum correlation coefficients. Table 1 shows the lag times for each of the events.

Another useful parameter in correlation analysis is the sample coefficient of determination which is the correlation coefficient squared (r^2). This represents the proportion of the variation in sound level explained by the regression of SL on RR, where SL is the sound intensity and RR is rainfall rate. That is, r^2 expresses the proportion of the total variation in the values of the sound intensity that can be accounted for or explained by a linear relationship with the rainfall rate.

B.   STORM EVENTS

A total of 22 individual events were recorded on the first two data tapes collected at NDBC's OTP during August and September of 1990. Table 1 lists the events, start times (CDST), run lengths and any time lag adjustment to the data records.

Most of the events were of a convective type associated with either a frontal system or local convective activity. From the radar images, some events can easily be confirmed as convective, especially in view of their precipitation rates. Other events either lack radar confirmation or had rainfall rates which could be classified as either convective or stratiform type precipitation.

C.   SOUND SPECTRUM WITH NO PRECIPITATION

When installing new data tapes, a manual test of the optical rain gauge trigger is preformed. During this test, the recording equipment is allowed to operate for 100 to 200 seconds. The data recorded during these tests contains wind generated sound spectra.

24

Table 1. Storm events.

Event	Start Time (CDST)	Original Length (sec)	Lag Time (sec)	Adjusted Length (sec)
900824A	22:44:50	1287	14	1273
900820B	23:06:58	451	0	451
900823	22:49:07	337	0	337
900824A	19:31:34	512	8	504
900824B	20:13:54	967	7	960
900824C	22:19:57	359	12	347
900824A	07:18:55	1238	21	1217
900824B	13:57:38	393	12	381
900830	17:16:33	493	22	471
900911A	17:09:18	640	21	619
900911B	17:48:03	1070	22	1048
900912A	00:00:15	372	3	409
900912B	05:27:22	870	14	854
900912C	05:43:51	870	0	379
900912D	07:15:04	425	16	409
900912E	08:18:34	339	14	325
900912F	18:43:10	738	15	723
900914A1	06:34:38	306	17	289
900914A2	06:40:30	374	0	374
900914B	08:49:52	419	0	409
900914C	09:03:31	459	0	409
900914D	09:19:03	457	31	426

Two events were recorded with no precipitation, one on 24 July 1990 and the other on

11 September 1990. In both cases, a "pure" wind spectrum was expected. Figure 16 is

a plot of sound level versus frequency for selected wind speeds from cases. With the
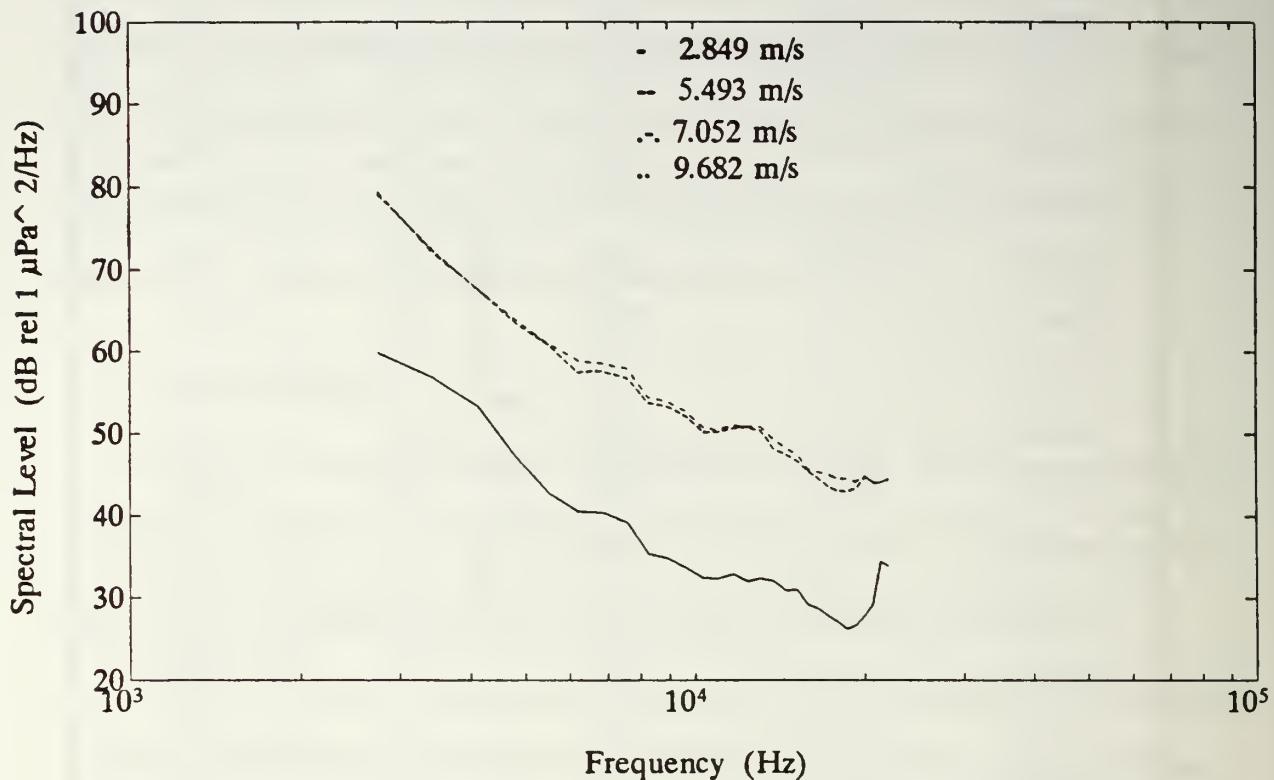
Figure 16. No rain cases from 24 July and 11 September 1990.

exception of the peaks located at approximately 7 and 13 kHz, the results are consistent

with Figure 1. The upturn at 20 kHz may be artificial due to the hydrophone sensitivity

(see Figure 9).

D. CHARACTERISTICS OF HEAVY CONVECTIVE PRECIPITATION

Large cumulus clouds are very dynamic, with strong vertical motions, and have very short development times (on the order of 30 minutes (thunderstorms) to that of tens of hours (supercells)). The water content of large cumulus clouds is high and rainfall rates exceeding 25 mm/hr are common. Convective rain produces large drop sizes early in its life cycle because of the processes by which strong upward vertical motion forces smaller drops upward or holds them aloft until significant growth in size is achieved by some process, normally collisions of the drops with each other. When this growth has occurred, the now large rain drops will overcome the upward vertical motion and fall to the surface. After the storm reaches maturity and the dissipation phase begins, the upward vertical motions weaken, allowing smaller drops to reach the earth's surface without as much growth occurring.

Figure 17 shows an instantaneous sound spectrum for 101.6 mm/hr. While some of the details of the spectrum, e.g., the peaks at 7 and 13 kHz and the levels below 5 kHz, are suspect due to the hydrophone sensitivity (see Figure 9), the general features of the spectrum from heavy rain can be described. The sound levels are very high when compared with the wind noise in Figure 1, implying that rain dominates the ambient sound field when it is present. The slope of the spectrum is not as steep as wind generated sound spectra. This supports the idea that rain and wind generated noise can be distinguished from each other by examining the slope of the shape of the underwater

27
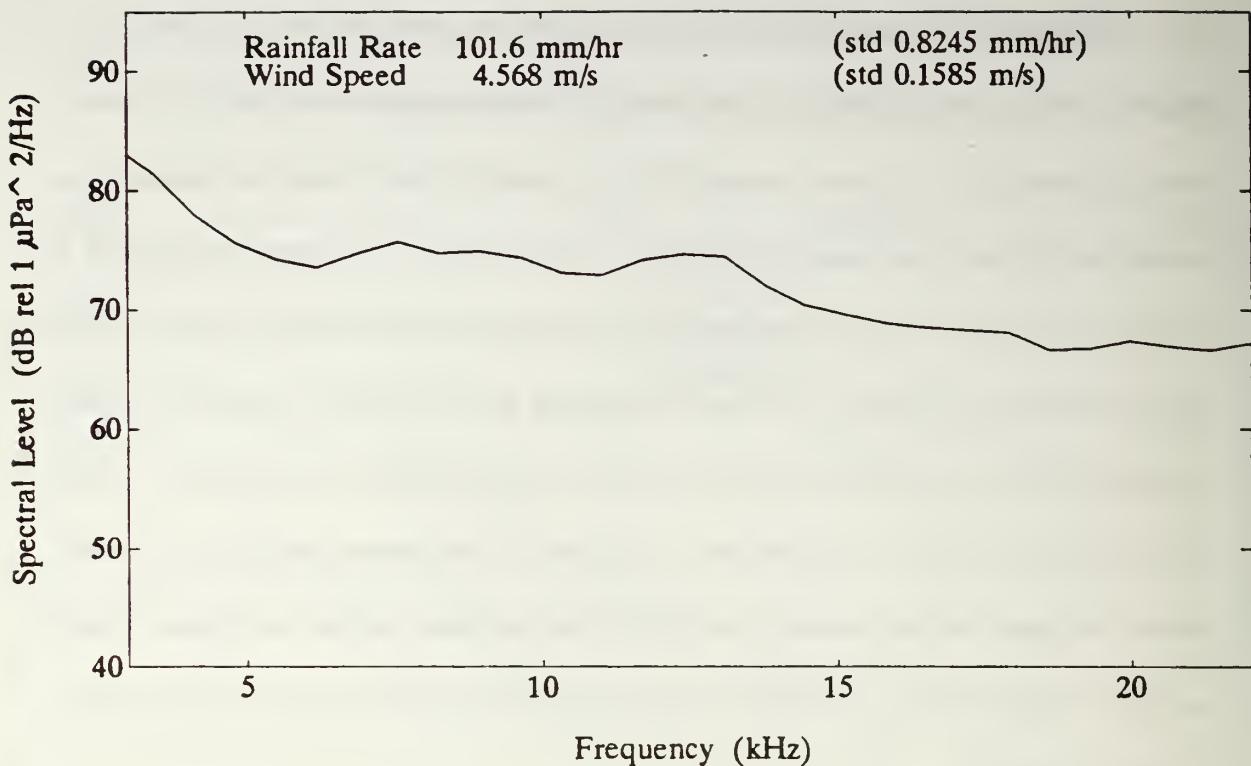
Figure 17. Example of a sound spectrum for heavy convective precipitation.

sound spectrum. Finally, no 15 kHz spectral peak is observed for heavy rainfall, contradicting Nystuen (1986).

To assess the influence of the changing character of the storm over the lifetime of the storm, time series of sound level at single frequencies were examined. Figure 18 shows a segment of data taken from 11 September 1990 when the wind speed was 4.85 m/s. At the rainfall rate of 70 mm/hr (vertical dashed line), the sound level when the rainfall rate was increasing was 73.5 dB rel 1 μPa^2/Hz and 70 dB rel 1 μPa^2/Hz when the rainfall rate was decreasing. Another example of this effect is taken from 14 September 1990 (Figure 19). Although on the scatter diagram, the sound levels during increasing

28
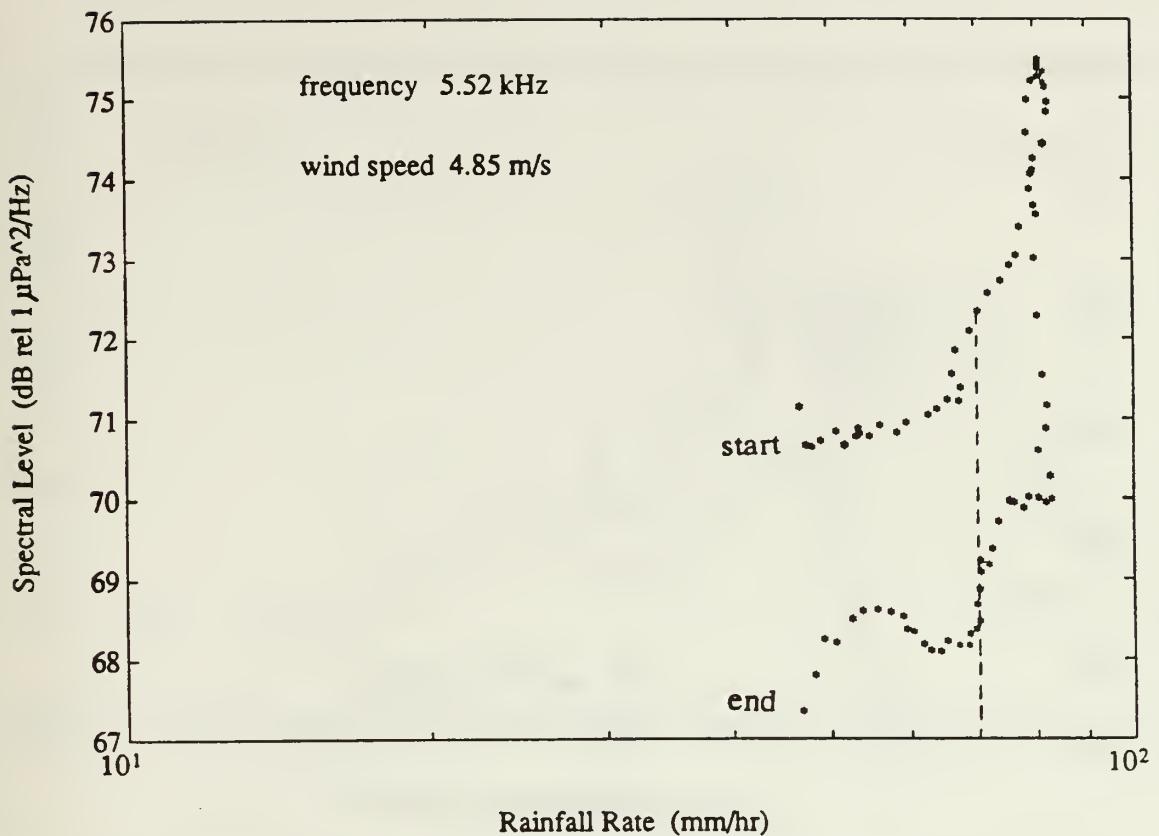
Figure 18. Segment of scatter plot from 11 September 1990 showing the difference in sound levels from the same rainfall rate. Each point represents one second of data. A rainfall rate of 70 mm/hr yields a sound level difference of 3.5 dB.

and decreasing rainfall rates approach each another, the sound level during increasing rainfall rate always remains above the sound level when the rainfall rate is decreasing. The difference in sound intensities reaches a maximum of 5.5 dB for a rainfall rate of 150 mm/hr.

Figure 20 shows a plot of an heavy convective event lasting 619 second on 11 September 1990, the distinct looping on the plot is characteristic of all the heavy convective events. The arrows drawn on Figure 20 show the progression of time. As the event starts, sound intensity increases with increasing rainfall rate (the wind at the

29
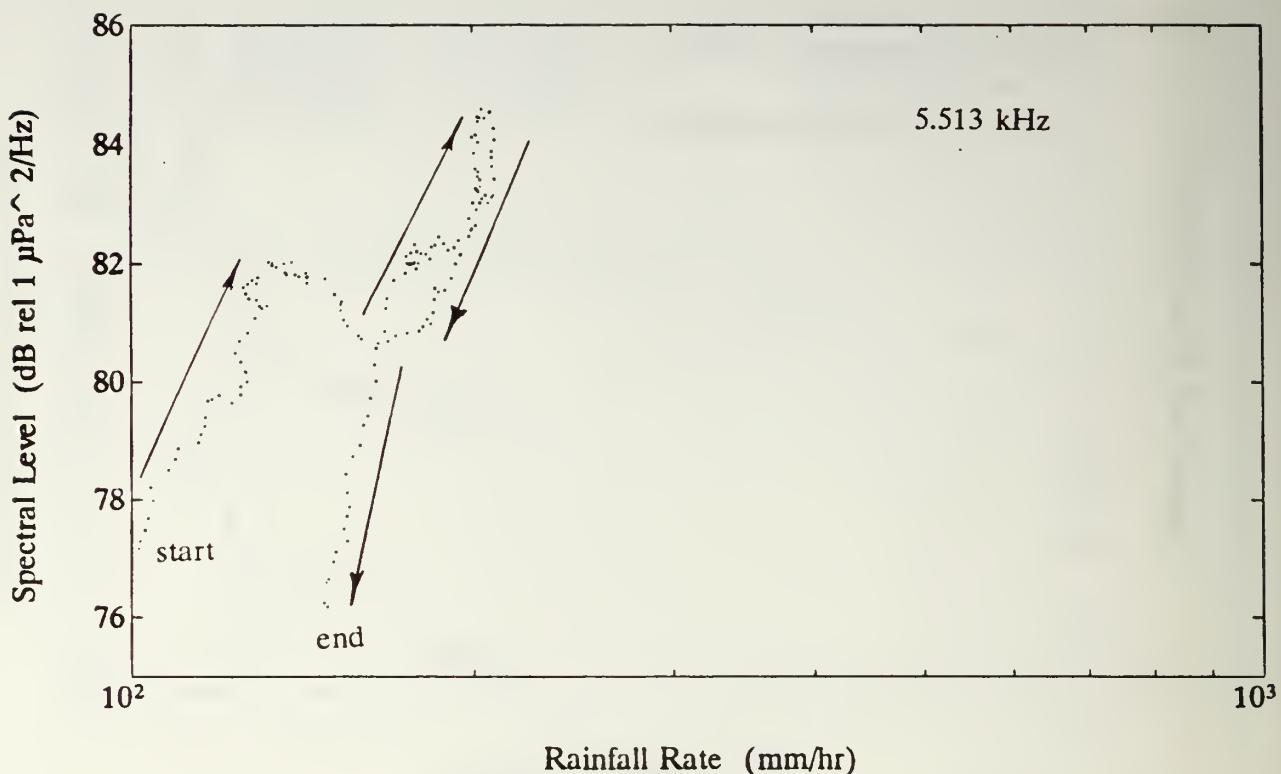
Figure 19. Segment of a scatter plot from 14 September 1990 showing sound level differences for high rainfall rates. The observed difference is 5.5 dB for a 150 mm/hr rainfall rate (wind speed is 6.17 m/s). Each point represents one second.

beginning of the time series is approximately 8 m/s and decreases to 4.5 m/s after 75 seconds). Subsequent arrows show lower sound levels for the same rainfall rate whenever the rainfall rate is decreasing. This feature continues throughout the event, always exhibiting the characteristic that the sound levels during increasing rainfall rate are higher than the sound levels for the same rainfall rate when the rainfall rate is decreasing.

Two possible explanations are suggested for this observation. The first being that at the start of rainfall, the drop size distribution is likely to consist of mostly larger drops (product of the strong upward vertical motions). Laboratory experiments (Snyder, 1990;
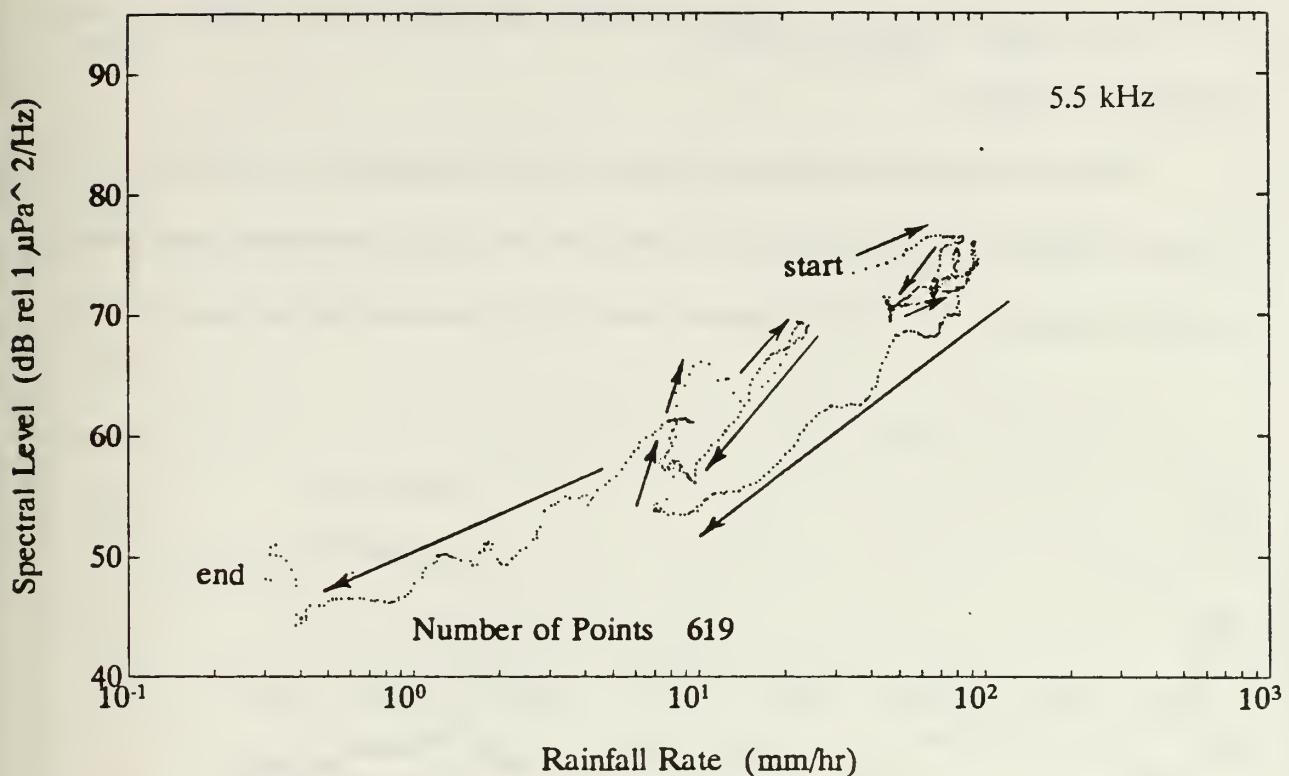
Figure 20. Scatter plot of the event on 11 September 1990. The looping within plot is attributed to increasing and decreasing rainfall rates within the storm. This phenomenon is observed in all heavy convective events. Frequency is 5.51 kHz.

Jacobus, 1991) have identified large drops (diameters 3 - 5 mm) as principal underwater sound producers. If these drops are present at the start of the rain, the sound levels will be higher than later in the rain when the rain volume has a larger proportion of smaller drops. The second possibility is that the temperature difference between the rain drop and the sea surface is largest at the start of the rainfall. A substantial temperature difference has been shown in the laboratory to significantly increase the sound intensity the bubble emits (Jacobus, 1991). As the rainfall continues, the sea surface temperature may change to more closely match the rain drop temperature. This may be due to mixing of the rain

31

water and the sea surface water or to the formation of a layer of rain water at the sea surface or perhaps because the formation altitude of raindrops can change over the lifetime of the storm.

Another characteristic of the sound spectra observed during heavy rainfall rates can be seen in Figure 21. This time series shows low and high frequencies sound levels parallel to each other (6 - 7 dB difference) until t = 260 seconds into the record. This is
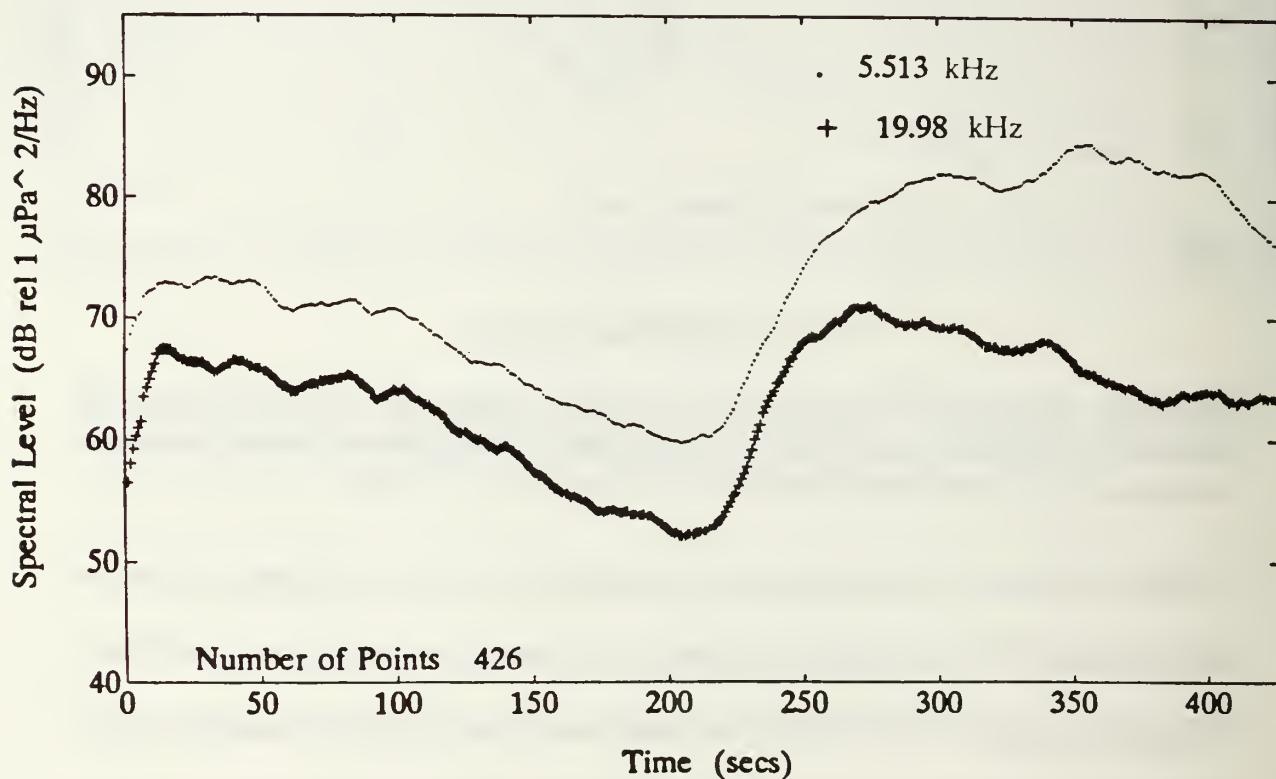
Figure 21. Storm event from 14 September 1990. Rainfall rates ranged from 50 to 210 mm/hr. Higher frequencies are suppressed due when heavy rain is presence suggesting the formation of a subsurface bubble cloud.

the time when the rainfall rate exceeds 125 mm/hr (Figure 22). As the high rainfall rates continues, the sound level at 5.51 kHz continues to follow the rainfall rate, however the
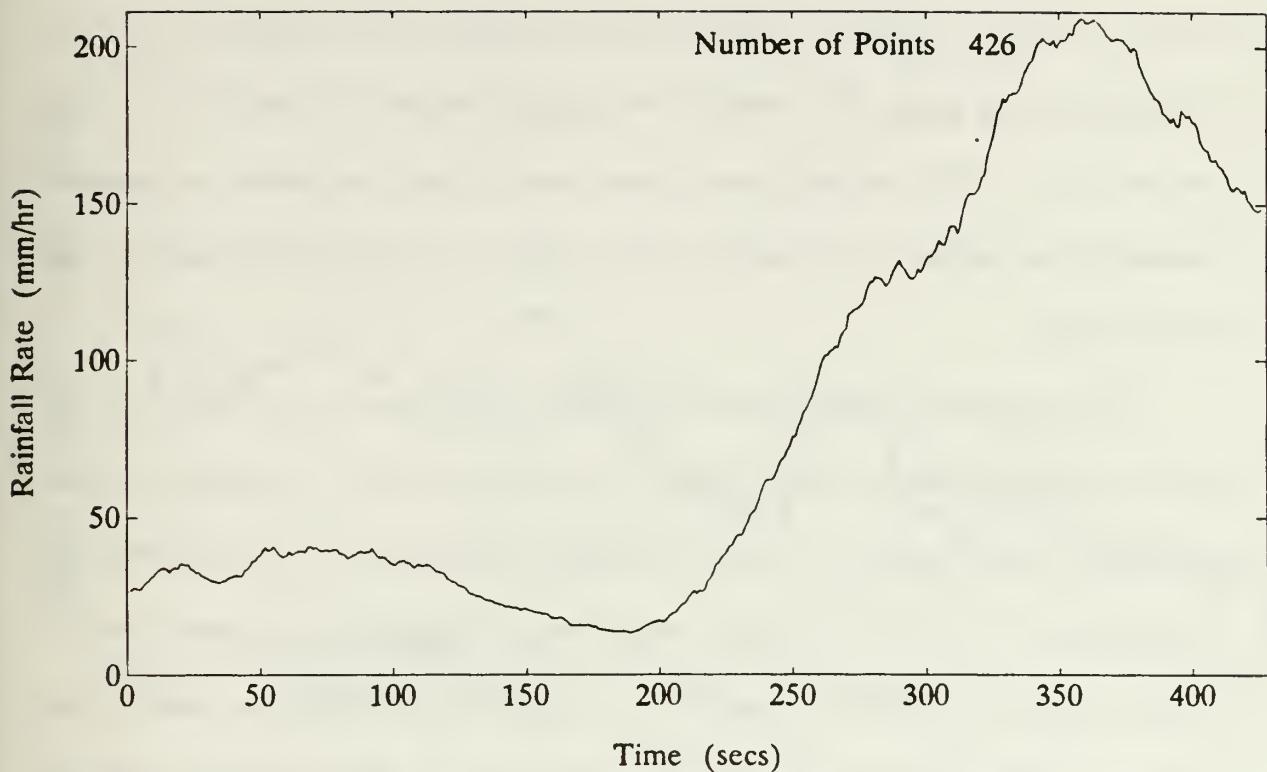
Figure 22. Rainfall rate time series from 14 September 1990.

high frequency sound level drops (spectral difference increases to 18 dB). This is

analogous to what is observed under very high wind speed conditions when bubble clouds

from breaking waves are thought to attenuate subsequent high frequency sound generated

at the surface (Farmer and Lemon, 1984) (i.e., new surface generated sound must

propagate through the bubble layer to reach the sound sensor and is attenuated while

doing so). The low frequencies are not affected as bubbles large enough to absorb low

frequency sound rapidly rise to the surface and are not part of an ambient subsurface

bubble cloud. In this case, the wind speed was 6 m/s, not fast enough to cause extensive

white capping. This observation suggests that rain itself is capable of creating a

33

subsurface bubble layer (and the associated subsurface mixing needed to stir the ambient bubbles downward). Figure 21 also provides information on the formation time of the subsurface bubble layer. The rainfall rate begins to exceed 125 mm/hr at t = 260 seconds. By t = 300 seconds, lower sound levels at high frequencies are evident, suggesting that bubble layer formation occurs within one minute of the onset of very heavy rainfall.

This suppression is only evident at very high rainfall rates (> 125 mm/hr for this study). At lesser rainfall rates, the spectral level differences ($SL_{5.5}$ - SL_{20}) generally does not exceed 10 dB (Figure 23). In cases where high rainfall rates are accompanied by high wind speeds (> 10 m/s), even stronger suppression of higher frequency sound levels is evident (e.g., event 900911B (Figure 24)). Figure 25 shows the time series of the environmental data (rainfall rate and wind speed) for this case. High wind (approximately 15 m/s) together with heavy rain (100 mm/hr) produced an observed spectral level difference of $SL_{5.5}$ - SL_{20} = 20 dB. As the wind died but the rainfall rate climbed to 200 mm/hr, the spectral level difference rose to a maximum of 35 dB. As the rainfall rate dropped, the spectral level difference returned to its typical value of less than 10 dB within one minute (delay could be caused by slow dissipation of the subsurface bubble cloud which continues to attenuate higher frequency sound after the rain has subsided). Occasionally, at the end of events the spectral level difference between 5.5 and 20 kHz crossed (see Figures 23 and 24). An examination (Figure 26) of the instantaneous sound spectra at t = 570 seconds in Figure 23 showed the 15 kHz spectral peak produced by the Type I bubble generation mechanism that has been previously observed under light rain
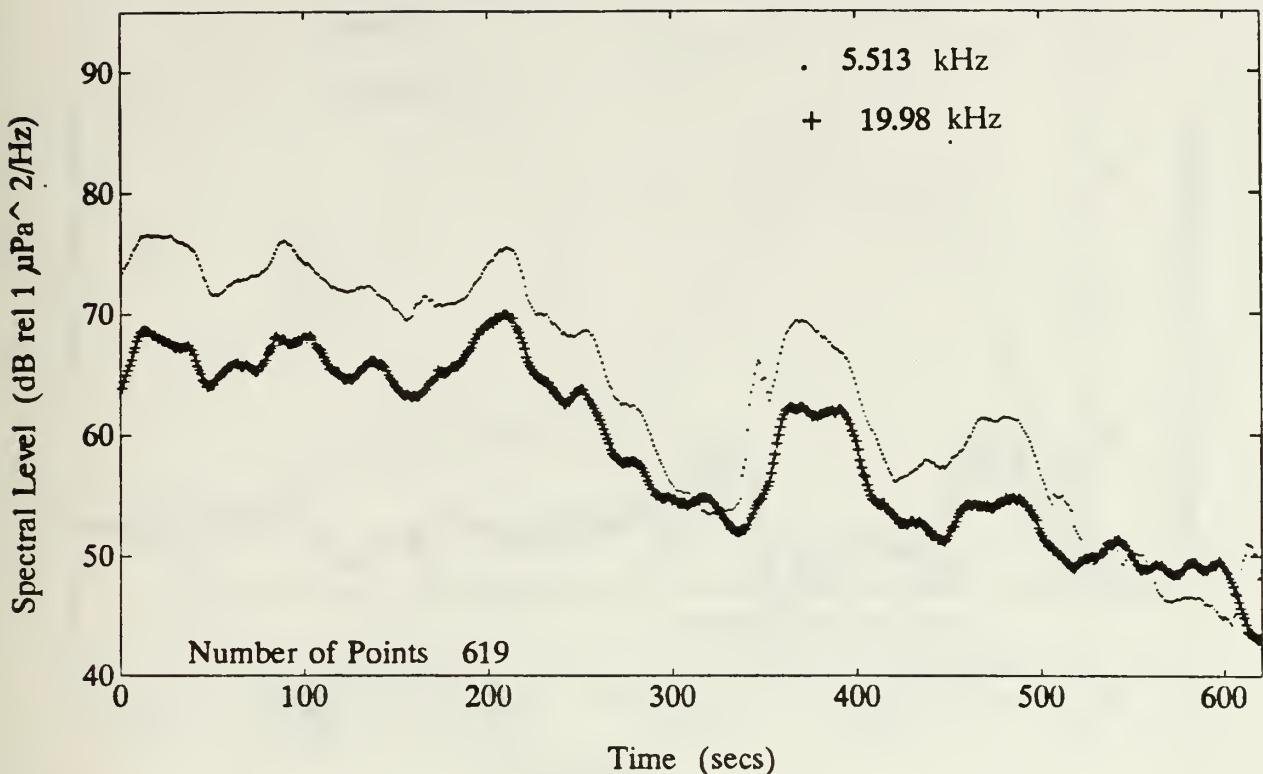
Figure 23. Time evolution of a storm event for 11 September 1990 showing no attenuation at higher frequencies. The rainfall rate ranged from 0 to 94 mm/hr and wind speed was initially 8 m/s (for first 75 seconds) and then decreased to 4.5 m/s.

and light wind conditions. At other times during these data when light wind conditions existed, no spectral peak was observed. Wind has been shown to suppress the Type I mechanism by roughing the ocean surface. Apparently heavy rain also suppresses this sound generation mechanism, probably by generating large ripples and thereby roughening the ocean surface.
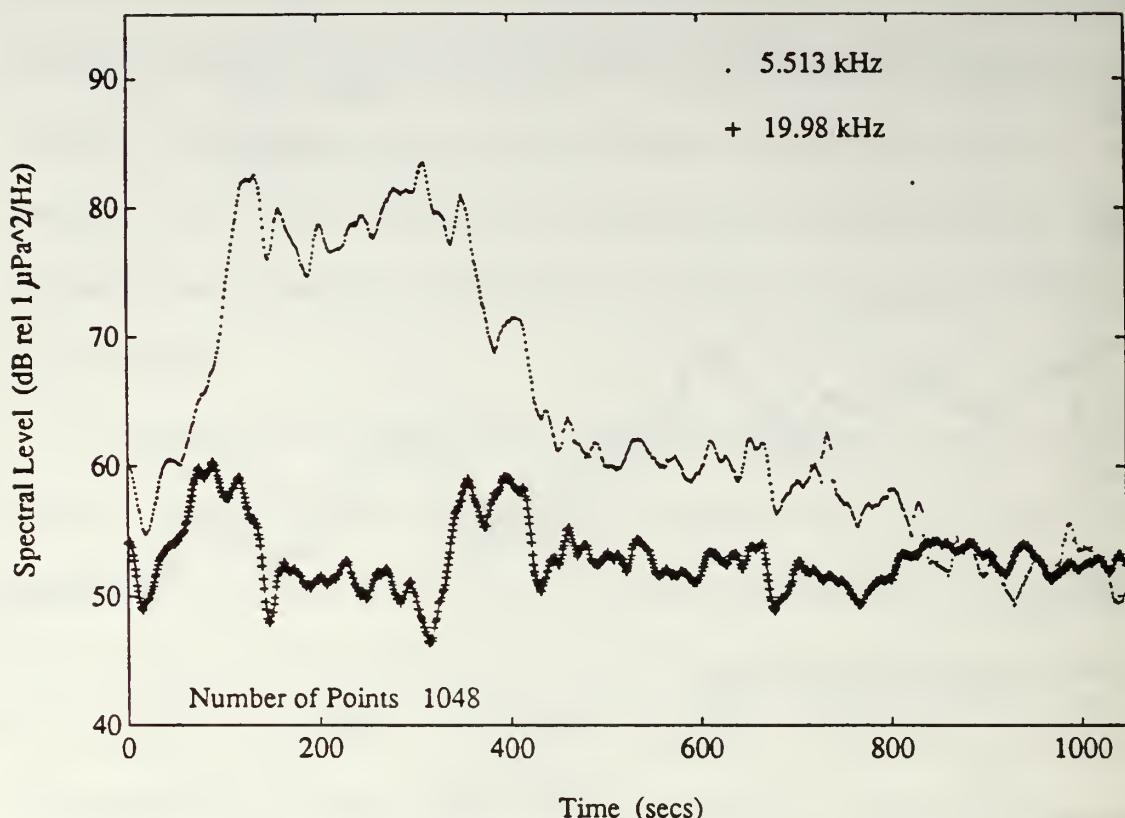
Figure 24. Strong suppression of higher frequencies (on 11 September 1990). Rainfall rate ranged from 100 to 221 mm/hr and wind speed was 15 m/s during the strongest suppression (see corresponding environmental data time series in Figure 25).

E. CHARACTERISTICS OF PRECIPITATION WITH RAINFALL RATES LESS THAN 50 MM/HR

Fifteen events were recorded when the rainfall rate was less than 50 mm/hr. Of these events, eleven had rates less than 25 mm/hr. The radar imagery failed to clearly classify any of the events as "pure" stratiform precipitation. One event (900823) based on rainfall rates and the uniformity of rainfall rate over time could possibility be classified as precipitation from a stratus cloud (no radar image for this period). All other events
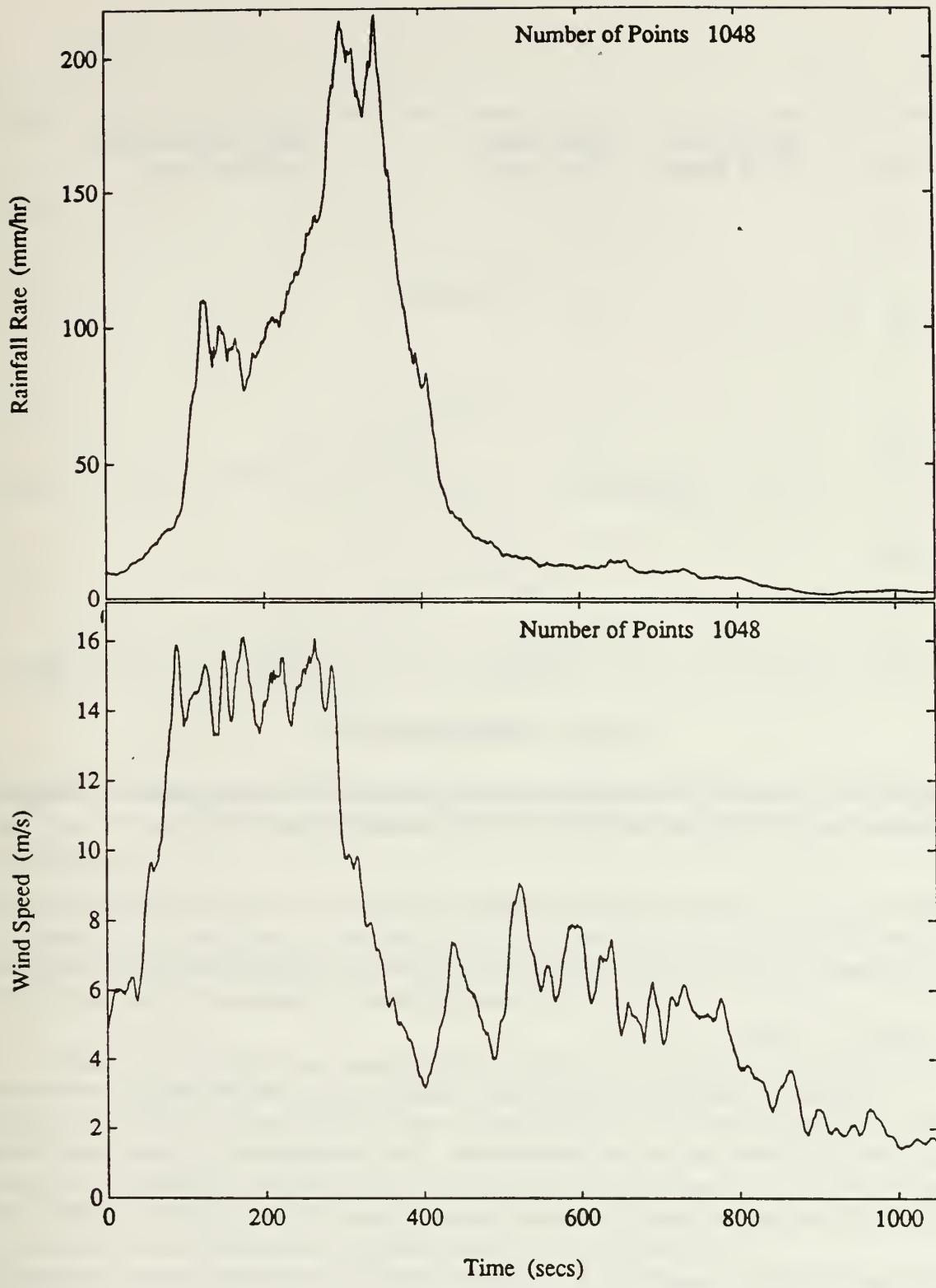
Figure 25. Time series of environmental data for the storm event on 11 September 1990. Rainfall rate (top plot) and wind speed (bottom plot) both contribute to the suppression of the spectral levels at higher frequencies in Figure 24.

37
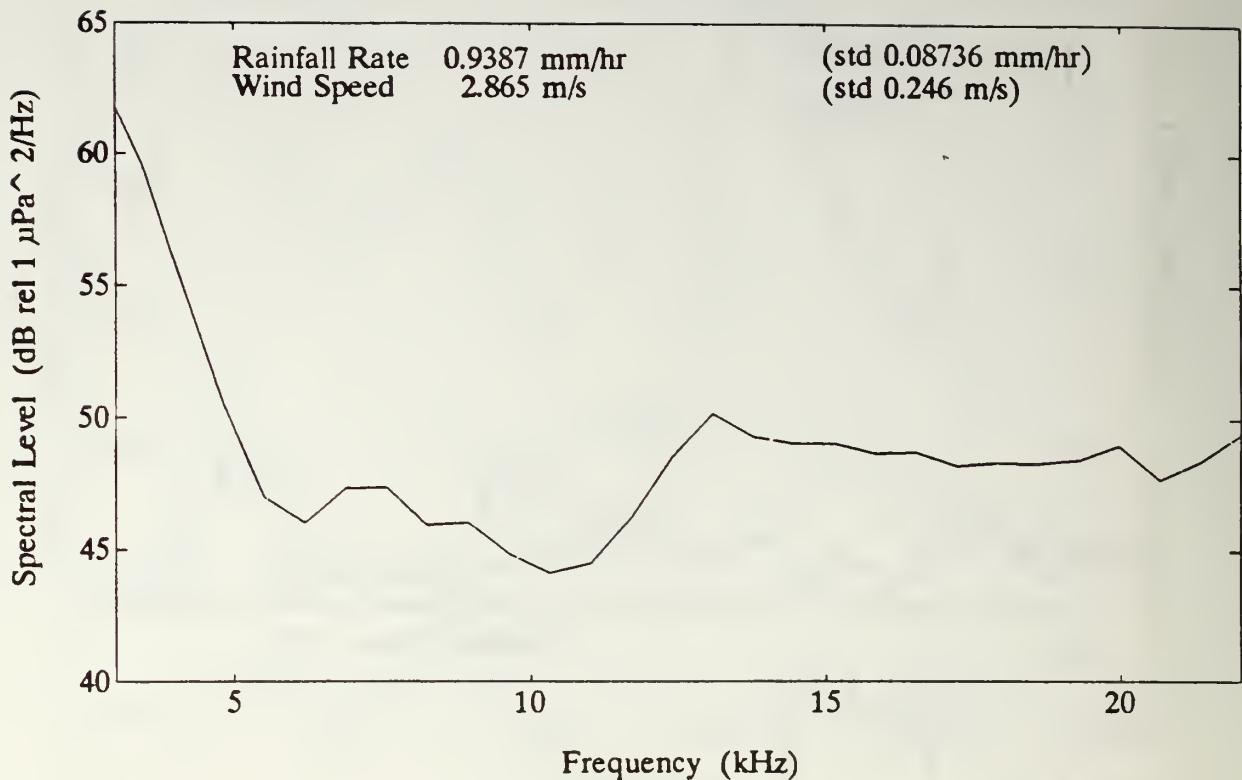
Figure 26. 15 kHz spectral peak under light rain and light wind conditions during the storm event on 11 September 1990 at t = 570 seconds (Figure 23).

were in areas or in close proximity to areas with convective activity. Subsequently the classification of these events were convective, when radar imagery clearly indicated such, or unknown origin.

The events classified as convective displayed many of the same characteristics described for heavy convective precipitation. The characteristic of sound levels being higher for increasing rainfall rate was present in many of the events but generally the difference between sound levels for increasing and decreasing rainfall at the same rainfall rate was smaller. Figure 27 is an convective precipitation event on 12 September 1990,

38
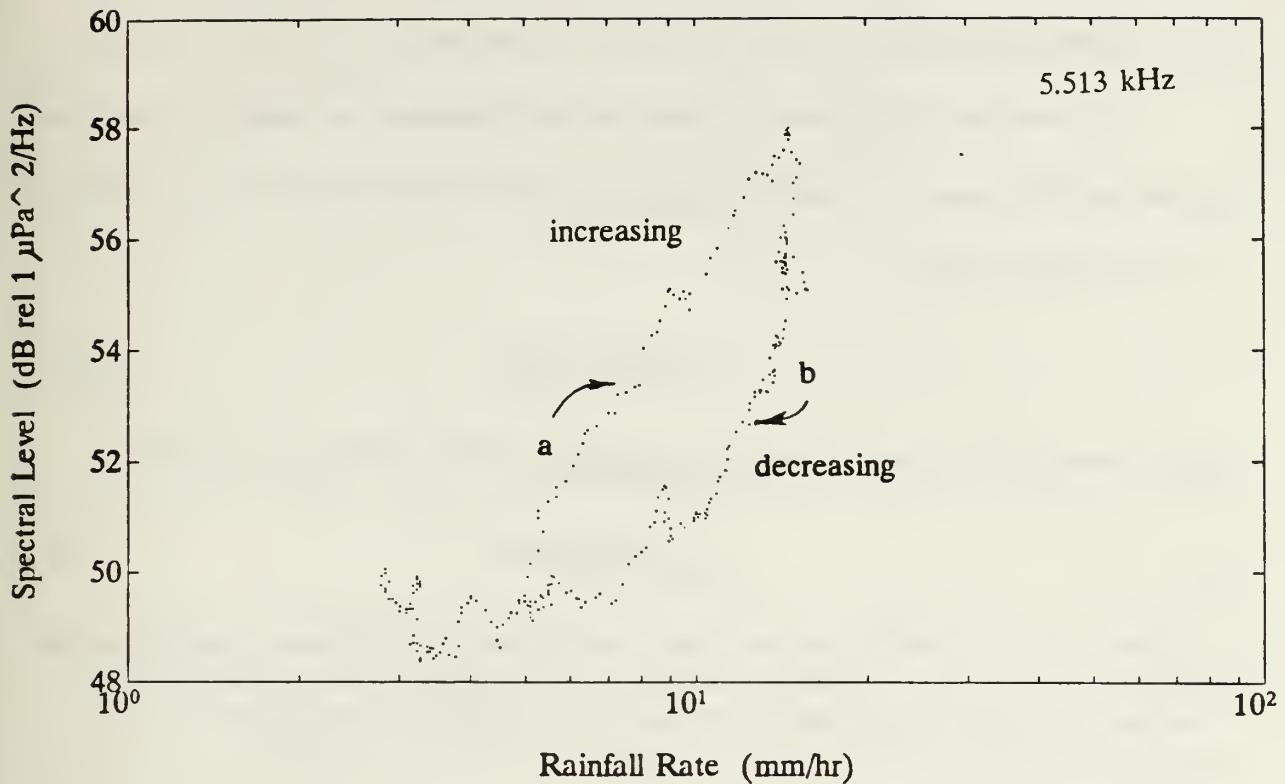
Figure 27. Scatter plot of sound intensity versus rainfall rate for a case with rainfall rates less than 50 mm/hr. Line (a) represents an increasing rate, line (b) represents the decreasing rate.

the rainfall rate is less than 16 mm/hr with a wind speed of 4 m/s for first 225 seconds of the time series, increasing to 6 m/s by the end of the series.

This event follows the same pattern as previously discussed for sound level differences between increasing and decreasing rainfall at the same rainfall rate. The sound level difference between the sound intensities from increasing (a) and decreasing (b) rainfall rate for this event is approximately 4 dB at 10 mm/hr.

F. CORRELATION COEFFICIENTS BETWEEN SPECTRAL LEVELS AND RAINFALL RATE

The correlation coefficient is a single number measuring the strength of the linear relationship between two variables. The relationship between the sound energy (SE) and the sound level (SL) is:

$$SL = 10 Log_{10}(SE) \tag{5}$$

If the sound level is proportional to the logarithm of the rainfall rate, the equation:

$$SL = a * Log_{10} RR + b \tag{6}$$

applies, RR is the rainfall rate and a and b are regression coefficients. This implies that the sound energy is proportional to the rainfall rate raised to some power.

$$SE = b^* * RR^{\frac{a}{10}} \tag{7}$$

Alternatively, the sound energy at a particular frequency is proportional to the number of drops of the size known to generate energy at that frequency (Jacobus, 1991). That is, sound energy $_{frequency}$ is equal to a constant (a*) times the number of drops of a given size. The most frequently used relationship for drop size distribution, the "Marshall-Palmer" distribution, is given by

$$DSD(d_0) = n_0 * e^{-\Lambda d_0} = n_0 * e^{-4.1 * RR^{-0.21} d_0} \tag{8}$$

where DSD is the drop size distribution (#/m³ mm), RR is the rainfall rate (mm/hr), Λ is slope factor (4.1 RR$^{-0.21}$ /mm), d_0 is drop size (mm) and n_0 is intercept parameter (8 x 10^3

40

/m³ mm) (Pruppacher and Klett, 1978). Assuming SE = a* DSD(d_0), using the Marshall-Palmer distribution for the number of drops, and taking 10 $\log_{10}$ of both sides, the result is

$$SL = b - a * RR^{-0.21} \tag{9}$$

where

$$b = 10 * \log_{10}(n_0 a^*) \tag{10}$$

$$a = 17.79 * d_0 \tag{11}$$

Both Equation (6) and Equation (9) were tried. Equation (9) produced a correlation coefficient of -0.84 at 5.5 kHz and Equation (6) produced 0.95 for the same frequency. Equation (9) produced a value of 0.086 for the associated slope which yields a drop diameter of 4.8 mm, this is consistent with large drop sizes in heavy rainfall. Correlation coefficients were slightly higher using Equation (6) for all frequencies, and so the following discussion considers the correlation of sound level and the logarithm of the rainfall rate.

1.   **Correlation Coefficients for Events with Maximum Rainfall Rates greater than 150 mm/hr**

Four cases of very heavy precipitation (> 150 mm/hr) were recorded (see Table 2 for environmental data). The correlation coefficient values are relatively high (> 0.85) for the lower to middle range of the frequency spectrum (4 to 15 kHz) and are

41

Table 2. Summary of environmental data for very heavy precipitation.

Event	Rainfall Rate (mm/hr)		Wind Speed (m/s)			
	max	min	max	min	μ	σ
900820A	344.44	1.61	9.15	0.00	4.59	2.37
900824B	290.12	0.33	18.38	2.48	6.31	3.01
900911B	216.12	1.58	16.12	1.43	7.09	4.39
900914D	209.35	13.33	8.88	3.74	6.68	1.14

measurably decreased for frequencies above 15 kHz (Figure 28). This result is consistent with the hypothesis that bubble clouds are produced by heavy rain, suppressing high frequency sound levels and producing lower correlation coefficients at high frequency. When high winds are also present, the correlation coefficient at high frequency approach zero.

When the sample coefficient of determination is computed, the amount of sound intensity that can be accounted for or explained by a linear relationship with rainfall rate is generated. This value for very high rainfall rates ranges from near zero for strong, sustained wind speeds at high frequencies (15 to 22 kHz) to 94.75% for moderate wind speeds (approximately 6 m/s) at low frequencies (< 10 kHz).
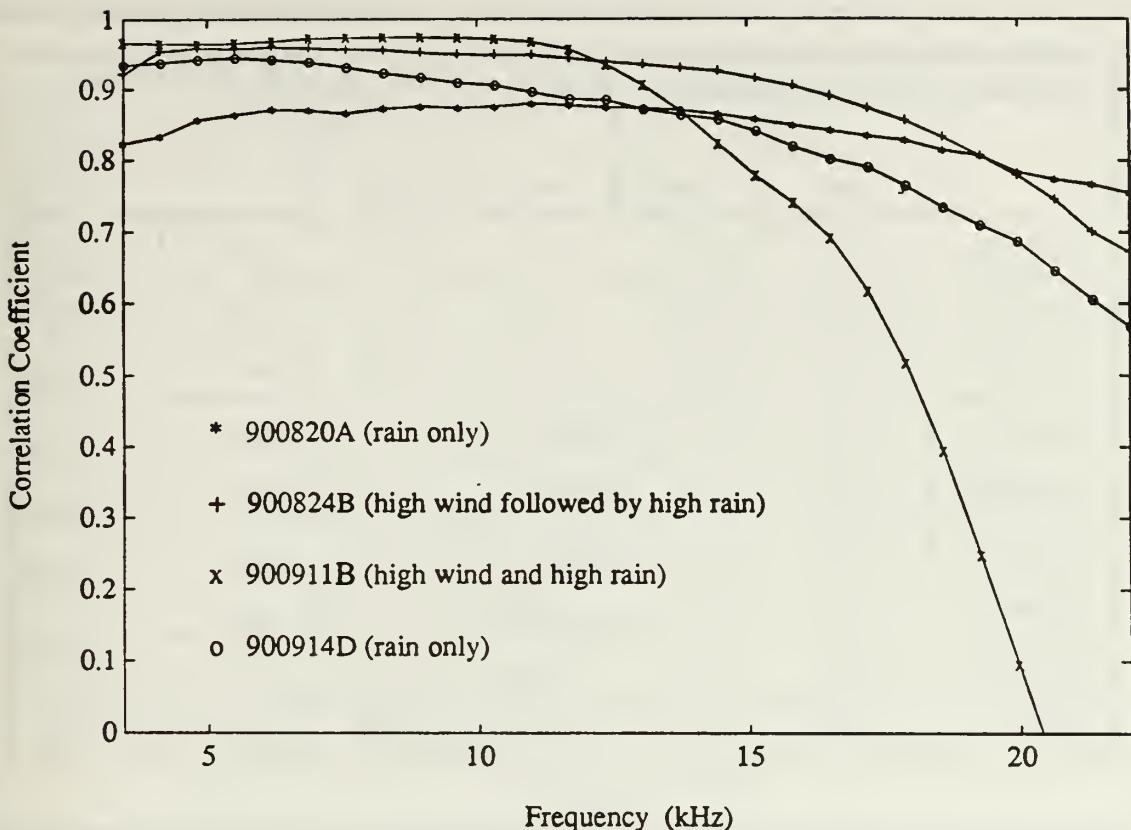
Figure 28. Correlation coefficients for sound level and rainfall rate for events with maximum rainfall rates greater than 150 mm/hr.

2. Correlation Coefficients for Events with Maximum Rainfall Rates less than 150 mm/hr and greater than 21 mm/hr

Nine events (Table 3) had maximum rainfall rates less than 150 mm/hr (the maximum rainfall rate was 105.19 mm/hr) and greater than 21 mm/hr. All of these cases had high values of correlation coefficients (Figure 29) at all frequencies. The wind speeds varied over the events but most had moderate wind speeds. All time series were at least 419 seconds in length. One event (900912B) that had high wind speeds (> 10 m/s) for a period of time (over 200 seconds) which appeared to effect the correlation

43

Table 3. Summary of environmental data for events with maximum rainfall rates less than 150 mm/hr and greater than 21 mm/hr.

Event	Rainfall Rate (mm/hr)		Wind Speed (m/s)			
	max	min	max	min	μ	σ
900824A	23.50	1.03	6.47	0.31	2.65	1.45
900827A	105.19	0.65	7.49	0.15	3.29	1.94
900830	50.67	8.66	18.79	10.96	14.74	1.82
900911A	96.37	0.30	9.51	2.53	4.84	1.24
900912B	61.83	0.98	14.08	2.83	6.89	3.61
900912D	42.19	0.18	9.09	4.84	7.28	0.81
900912F	32.51	0.19	11.85	3.42	8.62	1.70
900914B	23.62	0.36	4.86	1.31	3.05	0.81
900914C	25.80	0.18	9.97	2.39	4.81	1.69

coefficients (lowering the coefficient values at the upper frequencies). In one event (900912F), wind speeds greater than 10 m/s did not effect the correlation coefficients (event 900912F recorded wind speeds greater than 10 m/s, but was only present for approximately 100 seconds). One event (900830, Figure 30) had a mean wind speed of 14.74 m/s. The correlation coefficient for this event was between 0.85 and 0.9 for frequencies below 11 kHz and near 0.6 for higher frequencies. This is presumably a consequence of a subsurface bubble cloud generated by wave breaking because of the high winds.
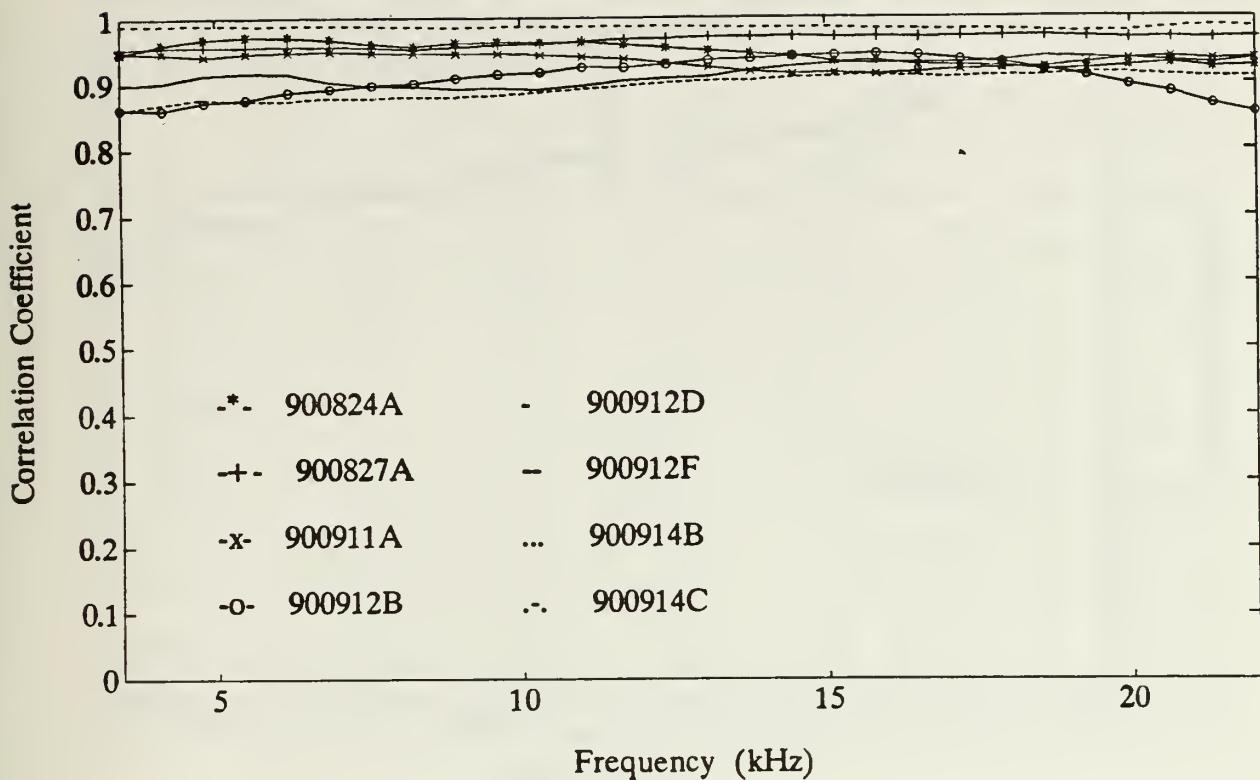
Figure 29. Correlation coefficients for sound level and rainfall rate for events with maximum rainfall rates less than 150 mm/hr and greater than 21 mm/hr. Wind speeds were moderate in all events (see Table 3).

3. Correlation Coefficients for Events with Maximum Rainfall Rates less than 21 mm/hr

Nine events had maximum rainfall rates less than 21 mm/hr (Table 4). These events had moderate to low wind speeds and produced varying correlation coefficients (Figure 31). All except one of the events (900820B) was less than 400 seconds in length. The low correlation coefficients could possibility be contributed to the short time series and/or low rainfall rates.

45
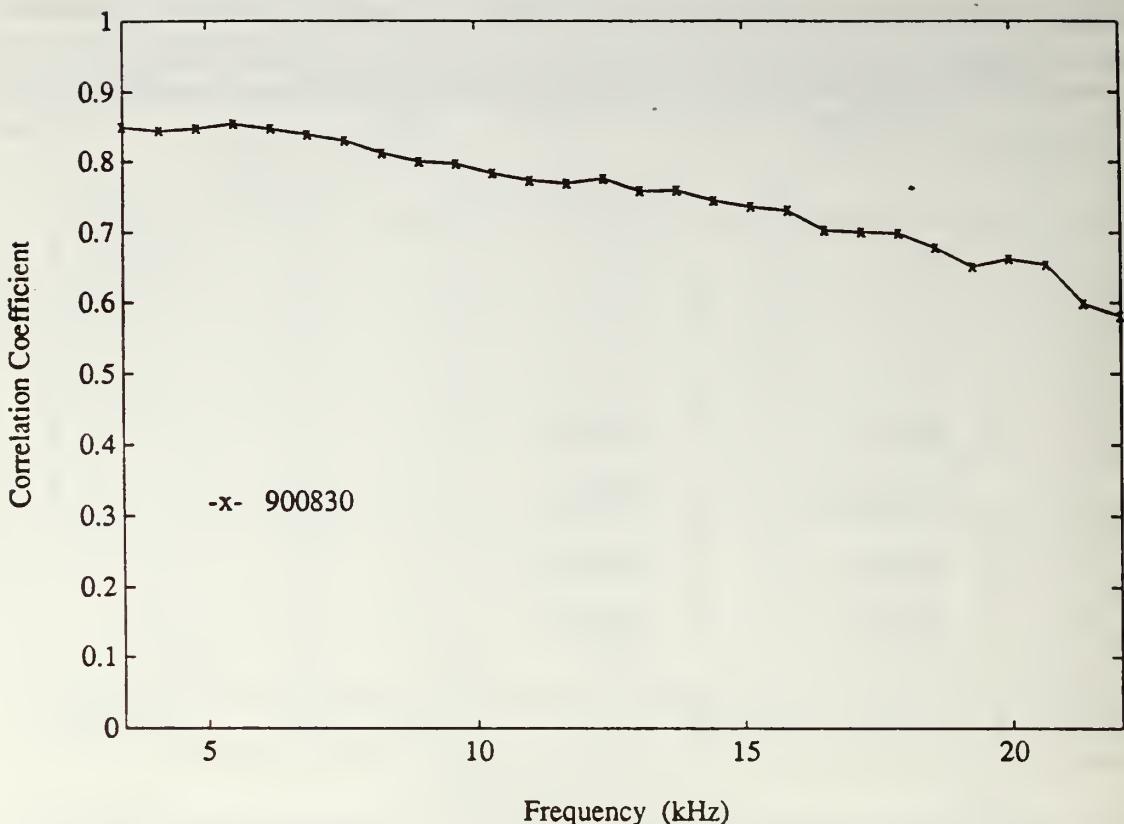
Figure 30. Correlation coefficients for sound level and rainfall rate for event 900830, which had a high wind speed (14.74 m/s).

G.   CORRELATIONS OVER MULTIPLE EVENTS

The events were divided into three main categories to look at the effects of wind during different precipitation conditions. The three groups were all precipitation events, events with maximum rainfall rates greater than 150 mm/hr and events with maximum rainfall rates less than 150 mm/hr. Each of these categories were divided into three wind speed subcategories, less than 5 m/s, between 5 and 10 m/s, and greater than 10 m/s. Correlation coefficients were calculated for each of these categories in order to better determine the relationship between multiple events.

46

Table 4. Summary of environmental data for events with maximum rainfall rates less than 21 mm/hr.

Event	Rainfall Rate (mm/hr)		Wind Speed (m/s)			
	max	min	max	min	μ	σ
900820B	17.64	0.93	7.72	4.61	6.24	0.65
900823	11.69	2.68	6.50	4.86	5.54	0.40
900824C	17.85	3.77	4.59	3.10	3.63	0.38
900827B	18.58	0.17	6.69	3.11	4.74	0.87
900912A	17.85	0.15	7.40	3.34	4.99	0.99
900912C	13.24	0.20	5.47	4.61	4.59	0.99
900912E	15.75	2.80	6.23	3.27	4.34	0.91
900914A1	10.23	1.26	5.24	1.81	3.85	1.00
900914A2	20.63	3.13	4.26	2.63	3.48	0.37

1. Precipitation Events with Maximum Rainfall Rates greater than 150 mm/hr

This category is composed of four events with very heavy rainfall rates (900820A, 900824B, 900911B and 900912D). The effects of the different wind speeds can be seen in Figure 32. The strong winds (> 10 m/s) have a significant effect on the correlation coefficients at the higher frequencies. For low wind speeds, the maximum correlation coefficient was 0.8828 at 12.40 kHz. The correlation coefficient values in the 5 to 10 m/s wind speed subcategories were the highest of the three subcategories with a maximum correlation of 0.9296 at 5.51 kHz. There were 350 data points (each data point
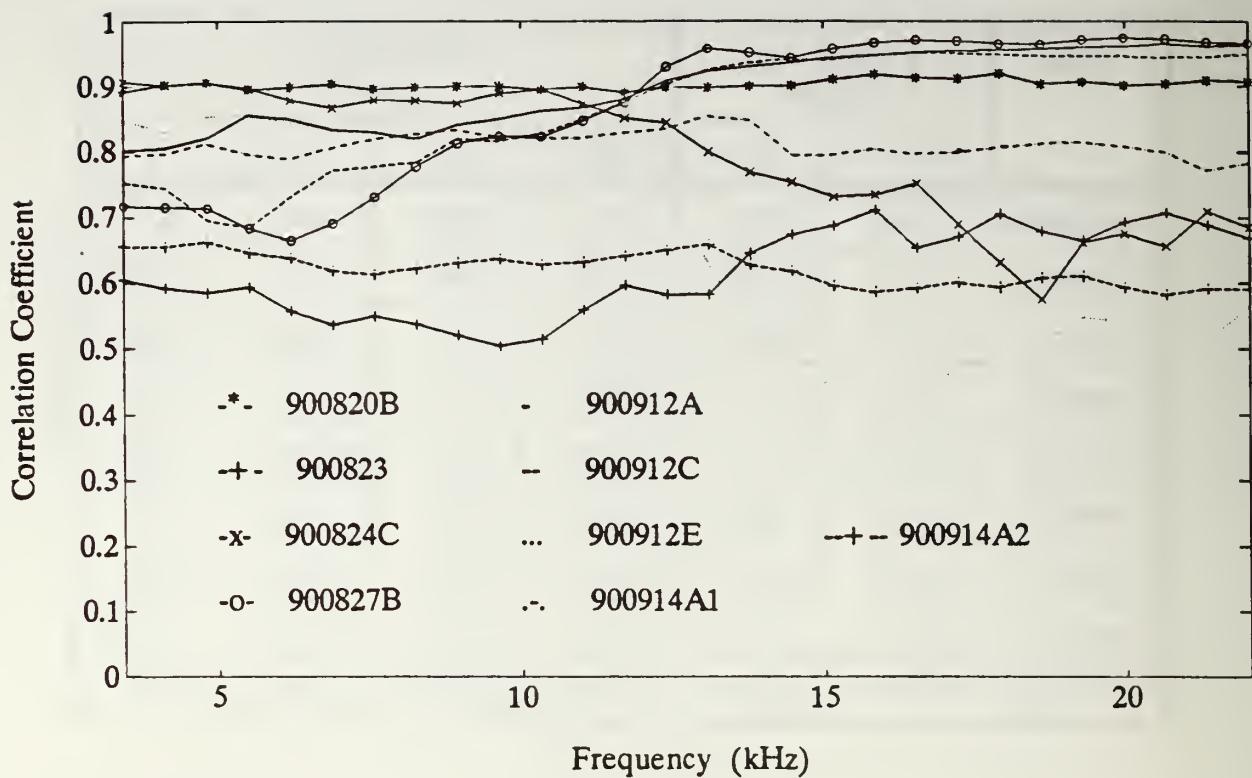
Figure 31. Correlation coefficients for sound level and rainfall rate for events with maximum rainfall rates less than 21 mm/hr. Wind speeds for all events were moderate (see Table 4).

is 1 second of real time) during the strong wind conditions (> 10 m/s), 1835 data points during moderate wind case (5 - 10 m/s) and 1522 data points during light wind conditions (< 5 m/s).

2.   **Precipitation Events with Maximum Rainfall Rates less than 150 mm/hr**

        Eighteen events comprised this category with rainfall rates ranging from 0.1932 to 105.15 mm/hr. At wind speeds less than 10 m/s, the correlation coefficients were higher at frequencies above 15 kHz (Figure 33). The best correlations were when the wind speed was less than 5 m/s. The majority of the data was taken when the wind speed

48
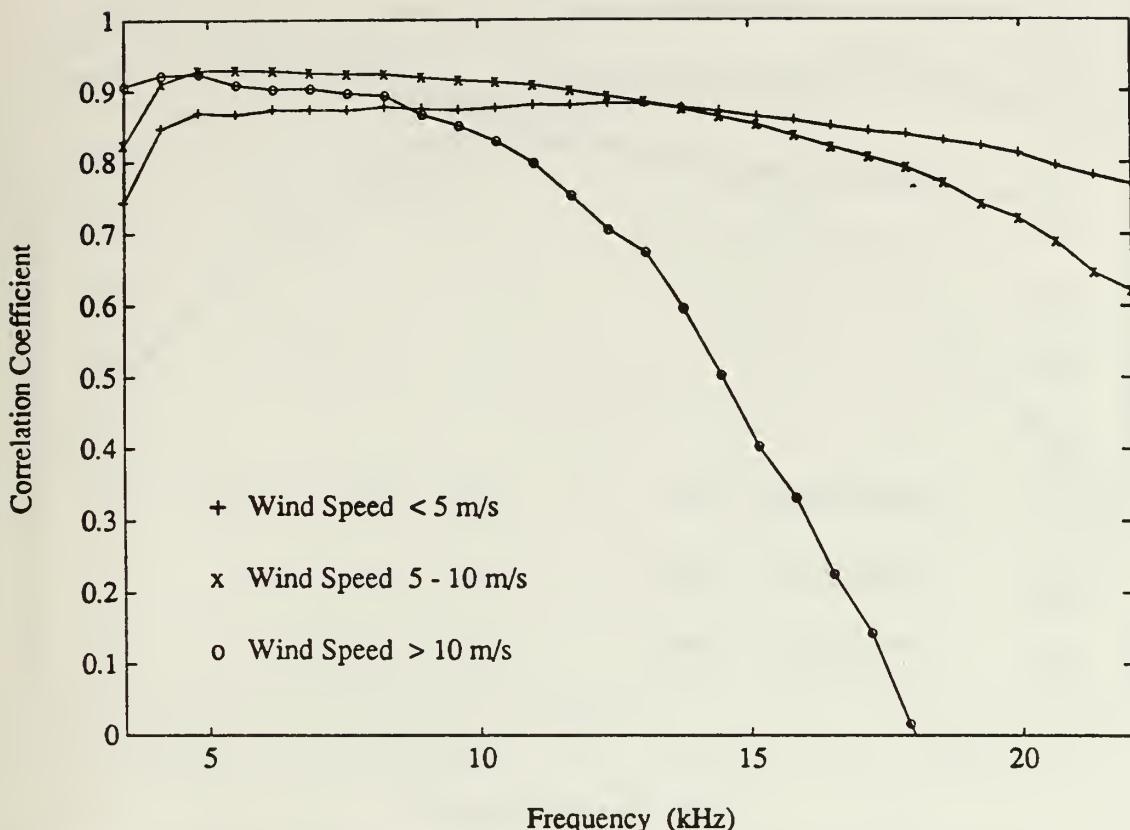
Figure 32. Correlation coefficients for sound level and rainfall rate for all events with maximum rainfall rates greater than 150 mm/hr for different wind speeds.

was less than 5 m/s (4981 data points). The effect of high wind strongly reduced correlation coefficients at high frequency.

3. All Precipitation Events

Figure 34 shows the correlation coefficients for all events in this study divided into subcategories of wind speed. For wind speeds less than 5 m/s there was 6503 data points, 4919 data points were recorded for the moderate wind speeds (5 - 10 m/s) and 1212 data points for the strong wind condition (> 10 m/s). To avoid the effects of
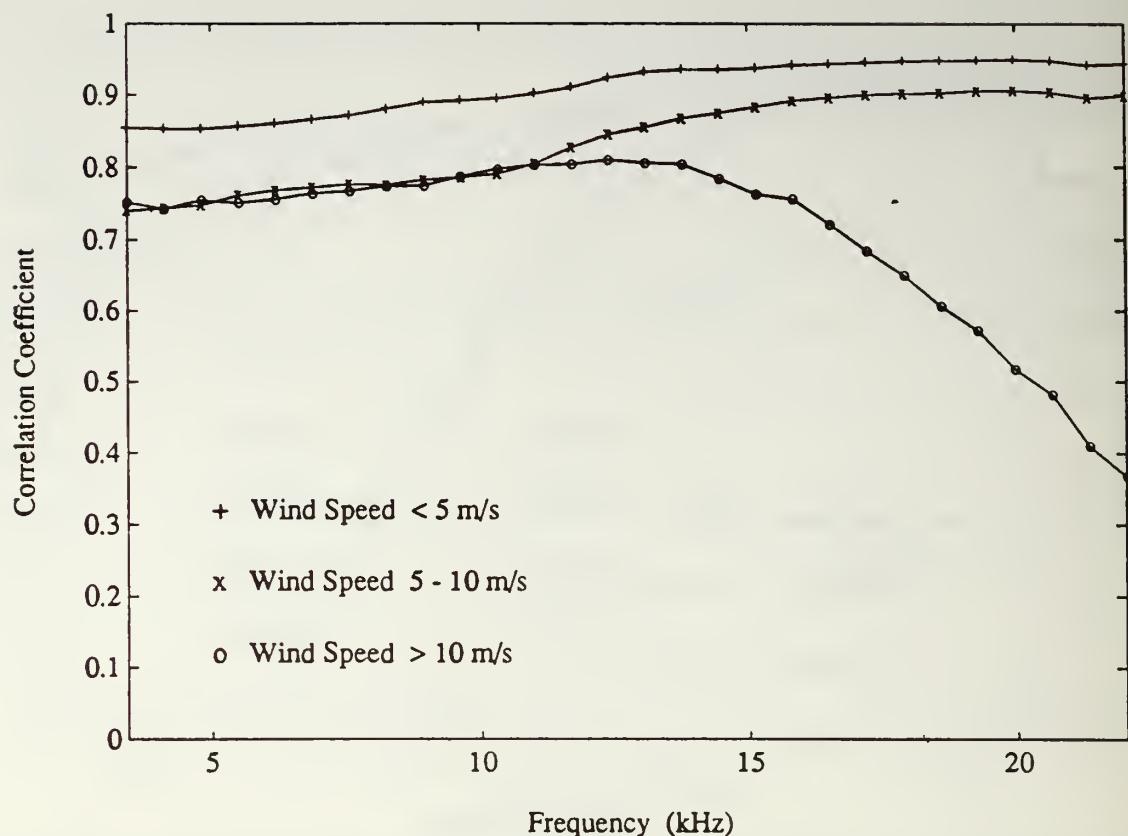
Figure 33. Correlation coefficients for sound level and rainfall rate for all events with maximum rainfall rates less than 150 mm/hr.

high wind and heavy rain, an empirical algorithm to predict rainfall rate from sound level

should use a frequency below 10 kHz.
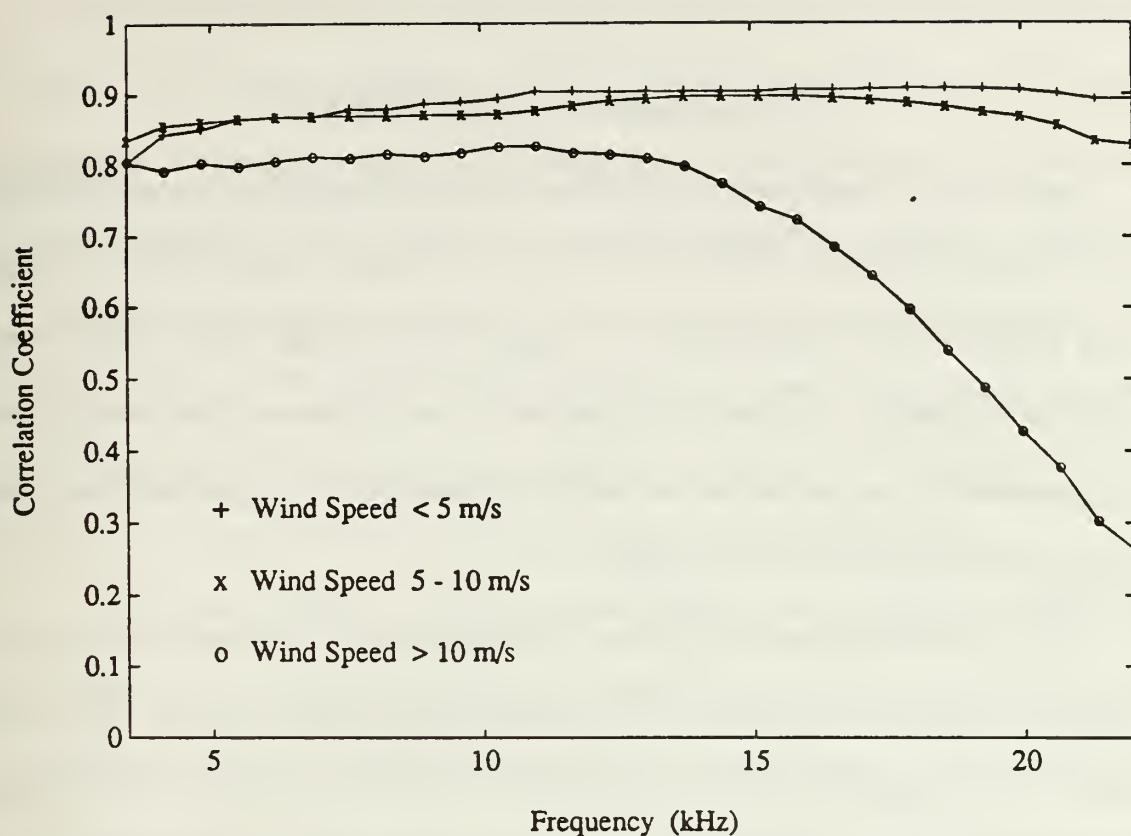
Figure 34. Correlation coefficients for sound level and rainfall rate for all events.

51

IV. SUMMARY AND DISCUSSION

In this study of underwater sound generated by heavy precipitation, several findings of importance are apparent. The fifteen kilohertz peak which has been studied extensively is not present in heavy precipitation; it is present only in light rain and light wind conditions (Figure 26). The wind is responsible for the suppression of the peak in light rain conditions by roughening the sea surface (Nystuen, 1990). Apparently heavy rain is equally able to roughen the sea surface.

Very high wind is known to generate a subsurface bubble cloud which modifies the observed underwater sound spectrum by attenuating high frequency sound. Heavy rain is apparently also capable of generating a subsurface bubble layer. When both high wind and heavy rain are present, the phenomenon is more intense. Unknown is the interaction between heavy rain and the wave breaking process.

An important feature of sound generated by heavy precipitation is that the sound level for the same rainfall rate changes during the storm cycle. At the beginning of the storm event and during increasing rainfall rates, the sound levels were notably higher than at the end of the storm event and for decreasing rainfall rates. This feature occurred in most events regardless of rainfall rate, although for the lesser rainfall rates, it was not as noticeable. Two possible explanations are suggested. The first being that during the life cycle of the storm event, the drop size distribution changes. In the beginning of the storm, the proportion of large drops is greater (Rogers and Yau, 1976) and as these drops

are most effective at producing sound (Snyder, 1990; Jacobus, 1991), the sound level is higher. The second explanation is that the sound energy produced by a drop is proportional to the difference in the temperatures between the drop and the ocean's surface (Jacobus, 1991). Early in a storm, this temperature difference is likely to be greatest. Later in the event, the ocean's surface may be closer to the temperature of the raindrops because of mixing of rain water and surface water (especially for very heavy rainfall). Alternatively, a layer of rain water may collect on the ocean's surface, also reducing the temperature difference between the rain and the sea surface.

Strong wind speeds (> 10 m/s) create breaking waves and bubbles which cause attenuation of the sound energy at higher frequencies and thereby reduce the correlation coefficients between sound level and rainfall rate at high frequency. This is also true of very heavy rainfall which suggests that the best frequencies to use for the measurement of rainfall rate by underwater sound are between 5 and 10 kHz. An empirical relationship between the sound level and the rainfall rate can be proposed. A linear regression line (Equation (12)) was fitted to 12,634 data points of varying rainfall rates and wind speeds at a frequency of 5.51 kHz. Note the slope of the regression (a = 10.59) which implies that sound energy is directly proportional to rainfall rate (Equation (7)). This empirical algorithm (rewritten as Equation (13)) suggests that sound energy is proportional to rainfall rate. However, no attempt has been made to adjust for changing conditions (i.e.,

$$SL_{5.5kHz} = 10.59 * Log_{10}RR + 53.29 \qquad (12)$$

drop size distribution, drop/surface temperature difference) during the lifetime of an event.

$$RR = 10^{\frac{SL_{s,sum} - 53.29}{10.59}}$$ (13)

When the algorithm is applied to a known data set, this shortcoming is clearly exhibited

(Figure 35). Errors in the algorithm associated with convective precipitation are the
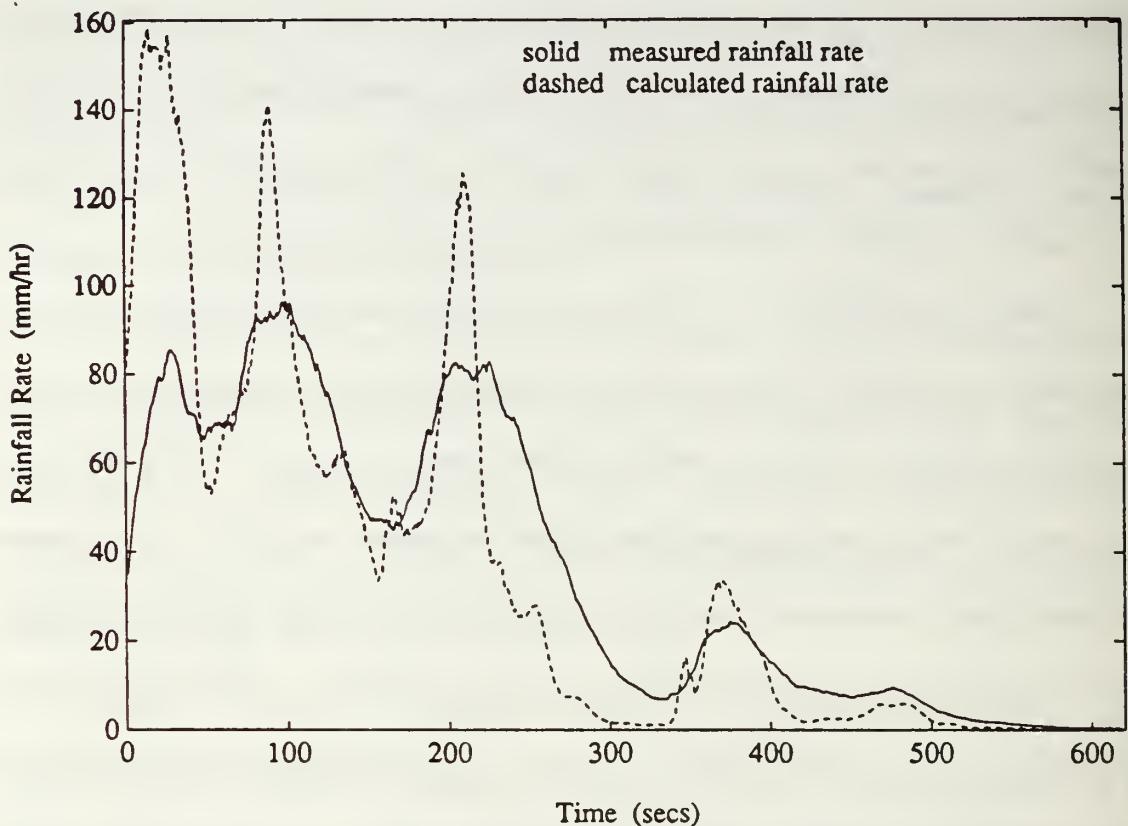
Figure 35. Proposed algorithm results when used on data with known rainfall rate. Overestimation and underestimation of rainfall rates reflect changing characteristics of heavy convective rain.

overestimation of rainfall rates at the beginning of the events and during increasing

rainfall rates and for very heavy rainfall rates (> 150 mm/hr). The algorithm

underestimates the rainfall rate at the end of the storm event and during decreasing

rainfall rates. Until there are refinements in the algorithm to include drop size

distribution (and temperature differences), this empirical algorithm for convective rainfall rate should be used cautiously.

V. CONCLUSIONS AND RECOMMENDATIONS

Rainfall measurement from underwater sound is still a relatively new idea; if successful, it will provide a means for acquiring environmental data remotely. This will be of great utility for better understanding of the atmospheric/oceanic heat balance processes. Twenty two events of convective rainfall were recorded at a coastal location during a two month period (August and September). The results show that the simplest view of just measuring sound intensity and inferring rainfall rate is not easily accomplished. Other factors such as drop size distribution and drop/sea temperature must be considered to accurately infer rainfall rate. The best correlation occurs at the higher frequencies for the storm events that have wind speed less than 10 m/s and rainfall rates less than 150 mm/hr. The suppression of sound at the higher frequencies is known to be caused by a subsurface bubble cloud created by the wind generated breaking waves. Very heavy rainfall rates are also observed to suppresses sound energy at the higher frequencies suggesting that heavy rainfall can form subsurface bubble clouds. The presence of these bubble clouds suggests that heavy rainfall produces subsurface mixing with subsequent influence on surface waves (Nystuen, 1990).

The conclusions are still tentative and additional data sets need to be analyzed over more events and during different seasons. In particular, rainfall from stratiform type cloud should be studied to see if there are differences when compared to convective precipitation. Future experiments should attempt to include drop size distributions of the

rain to help achieve a better understanding of the ambient noise generated by rain and to allow the effect of variable drop size distribution to be incorporated into future rainfall rate algorithms.

LIST OF REFERENCES

Evans D.L., Watts D.R., Halpern D., and Bourassa S., "Oceanic Winds Measured from the Sea Floor", J. Geophys. Res., **89**, 3457-3461, 1984.

Farmer D.M. and Lemon D.D., "Acoustic Measurement of Wind Speed and Precipitation over a Continental Shelf", J. Geophys. Res., **89**, 3462-3472, 1984.

Farmer D.M. and Vagle S., "On the Determination of Breaking Surface Wave Distributions Using Ambient Sound", J. Geophys. Res., **93**, 3591-3600, 1988.

Jacobus, P.W., "Underwater Sound Radiation from Large Raindrops", MS Thesis, Naval Postgraduate School, Monterey, CA,1991; (To be published in September 1991).

Knudsen V.O., Alford R.S., and Emling J.W., "Underwater Ambient Noise", J. Marine Res. **1**, 410-429, 1948.

Kurgan A., "Underwater Sound Radiated by Impacts and Bubbles Created by Raindrops", M.S. Thesis, Naval Postgraduate School, Monterey, CA, 1989.

Medwin H. and Beaky M.M., "Bubble Sources of the Knudson Sea Noise Spectra", J. Acoust. Soc. Amer., **86**, 1124-1130, 1989.

Medwin H., Kurgan A., and Nystuen J. A., "Impact and Bubble Sound from Raindrops at Normal and Oblique Incidence", J. Acoust. Soc. Amer.,**88**, 413-418, 1990.

Nystuen J.A., "Rainfall Measurements Using Underwater Sound Ambient Noise", J. Acoust. Soc. Amer., **79**, 972-982, 1986.

Nystuen J.A. and Farmer D.M., "The Influence of Wind on the Underwater Sound Generated by Light Rain", J. Acoust. Soc. Amer., **82**, 270-274, 1987.

Nystuen J.A. and Farmer D.M., "Precipitation in the Canadian Atlantic Storms Program: Measurements of the Acoustic Signature", Atmosphere-Ocean, **27**, 237-257, 1989.

Nystuen J.A., "A Note on the Attenuation of Surface Gravity Waves by Rainfall", J. Geophys. Res., **95**, 18353-18355, 1990.

Nystuen J.A., "An Explanation of the Sound Generated by Light Rain in the Presence of Wind", *Natural Sources of Underwater Sound*, B. R. Kerman, Kluwer Academic Press, 1991.

Pruppacher H.R. and Klett J.D., *Microphysics of Clouds and Precipitation*, D. Reidel Publishing Company, 714 pp., 1978.

Pumphrey H.C., Crum L.A. and Bjorno, L., "Underwater Sound Produced by Individual Drop Impact and Rainfall", J. Acoust. Soc. Amer., **85**, 1518-1526, 1989.

Pumphrey H.C. and Crum L.A., "Free Oscillations of Near-Surface Bubbles as a Source of the Underwater Noise of Rain", J. Acoust. Soc. Amer., **87**, 142-148, 1990.

Rogers R.R. and Yau M.K., *A Short Course in Cloud Physics*, Pergamon Press, 293 pp., 1976.

Scrimger J.A., Evans D.J. and Yee W., "Underwater Noise Due to Rain - Open Ocean Measurements", J. Acoust. Soc. Amer., **85**, 726-731, 1989.

Snyder D.E., "Characteristics of Sound Radiation from Large Raindrops", MS Thesis, Naval Postgraduate School, Monterey, CA, 1990.

Tan C.L., "A Characterization of Underwater Sound Produced by Heavy Precipitation",
M.S. Thesis, Naval Postgraduate School, Monterey, CA, 1990.

Vagle S., Large W.G. and Farmer D.M., "An Evaluation of the WOTAN Technique of
Inferring Oceanic Winds from Underwater Ambient Sound", J. Atmos. and Oceanic
Tech., 7, 576-595, 1990.

INITIAL DISTRIBUTION LIST

6. Dr. H. Medwin   1

    Code (PH/Md)

    Naval Postgraduate School

    Monterey, CA 93943-5000

7. Commander   1

    Naval Oceanography Command

    Stennis Space Center

    MS 39529-5000

8. Commanding Officer   1

    Fleet Numerical Oceanography Center

    Monterey, CA 93943-5005

9. Commanding Officer   1

    Naval Oceanographic and Atmospheric Research

    Laboratory

    Stennis Space Center

    MS 39529-5004

10. Office of Naval Research (Code 420)   1

    Naval Ocean Research and Development Activity

    800 N. Quincy Street

    Arlington, VA 22217

11. Mr. Harry Selsor   1

    Code 311, NOARL

    Stennis Space Center

    MS 39529-5004

12. Lt. Charles C. McGlothin, USN   1

    Department Head School (Class 120)

    Surface Warfare Officer School Command

    Newport, RI 02841-5012